THE SUBSTRATE AND REGULATOR OF ACETYLTRANSFERASE SAN

APPROVED BY SUPERVISORY COMMITTEE

Hui Zou, Ph.D.

Zhijian J. Chen, Ph.D.

Eric Olson, Ph.D.

Woodring Wright, M.D., Ph.D.

TO MY BELOVED PARENTS AND BROTHER

THE SUBSTRATE AND REGULATOR OF ACETYLTRANSFERASE SAN

by

CHIH-WEN CHU

DISSERTATION

Presented to the Faculty of the Graduate School of Biomedical Sciences

The University of Texas Southwestern Medical Center at Dallas

In Partial Fulfillment of the Requirements

For the Degree of

DOCTOR OF PHILOSOPHY

The University of Texas Southwestern Medical Center at Dallas

Dallas, Texas

May, 2010

THE SUBSTRATE AND REGULATOR OF ACETYLTRANSFERASE SAN

CHIH-WEN CHU, Ph.D.

The University of Texas Southwestern Medical Center at Dallas, 2010

HUI ZOU, Ph.D.

Lysine acetylation is one of the most common protein modifications in eukaryotes and plays critical roles in numerous cellular events. San is an acetyltransferase required for proper chromosome segregation in *Drosophila* and human, but little is known about its substrates or upstream regulators. To identify San substrates, I performed affinity purification and demonstrated that tubulin is a San substrate. Tubulins are the building blocks of microtubules, which display dynamic instability. By regulating the rate of microtubule assembly and disassembly, cells organize the microtubule cytoskeleton to accommodate their specific functions. Posttranslational modifications of tubulin have

been implicated in regulating microtubule functions. San acetylates β-tubulin on lysine-252, which only occurs on free tubulin heterodimers. The acetylation-mimicking mutants are incorporated into the microtubule cytoskeleton in HeLa cells without causing any obvious microtubule defect. However, after cold-induced catastrophe, microtubule regrowth is accelerated in San-siRNA cells while the incorporation of the acetylation-mimicking mutant tubulins is severely impeded. The lysine-252 of β-tubulin localizes at the intradimer interface and interacts with the phosphate group of the α-tubulin-bound GTP. Based on these findings, I propose that San regulates tubulin polymerization by acetylating β-tubulin lysine-252, which neutralizes the positive charge and makes the tubulin heterodimer adopt a conformation that disfavors tubulin polymerization. In addition, I present evidence indicating that the enzymatic activity of San is inhibited by a protein in an ATP-dependent but hydrolysis-independent manner. Purification and identification of this San inhibitor is still under way, and preliminary data from gel filtration chromatography suggest that the inhibitor may be a multi-subunit protein complex.

TABLE OF CONTENTS

PRIOR PUBLICATIONS

Hou, F., Chu, C.W., Kong, X., Yokomori, K., and Zou, H. (2007). The acetyltransferase activity of San stabilizes the mitotic cohesin at the centromeres in a shugoshin-independent manner. *J Cell Biol* 177, 587-597.

Chu, C.W., Hou, F., Zhang, J., Phu, L., Loktev, A.V., Kirkpatrick, D.S., Jackson, P.K., Zhao, Y., and Zou, H. (2010). A novel acetylation of β-tubulin by San modulates microtubule polymerization via down-regulating tubulin incorporation. *Under revision.*

LIST OF FIGURES

LIST OF TABLES

LIST OF ABBREVIATIONS

NAT – N-acetyltransferase

KAT – lysine acetyltransferase

KDAC – lysine deacetylase

GNAT – Gcn5-related N-acetyltransferase

DNA – deoxyribonucleic acid

SAGA – Spt-Ada-Gcn5 acetyltransferase

STAGA – Spt3-TAF9-GCN5/PCAF acetyltransferase

ATAC – Ada-two-A-containing

MT – microtubule

MTOC – microtubule organizing center

GTP – guanosine-5'-triphosphate

GDP – guanosine-5'-diphosphate

MAP – microtubule-associated proteins

ATP – adenosine-5'-triphosphate

+TIP – microtubule plus-end tracking protein

CTT – C-terminal tail

DAPI – 4',6-diamidino-2-phenylindole

CHAPTER ONE

GENERAL INTRODUCTION

1.1 Acetyltransferase

Acetylation is an enzyme-catalyzed reaction involving transfer of an acetyl group from acetyl-CoA to an amino group, resulting in removal of the positive charge. Depending on the position of the amino group within an amino acid, acetylation events can be divided into two types: N-terminal acetylation (N^{α}-acetylation) and lysine acetylation (N^{ε}-acetylation) (Fig. 1.1).

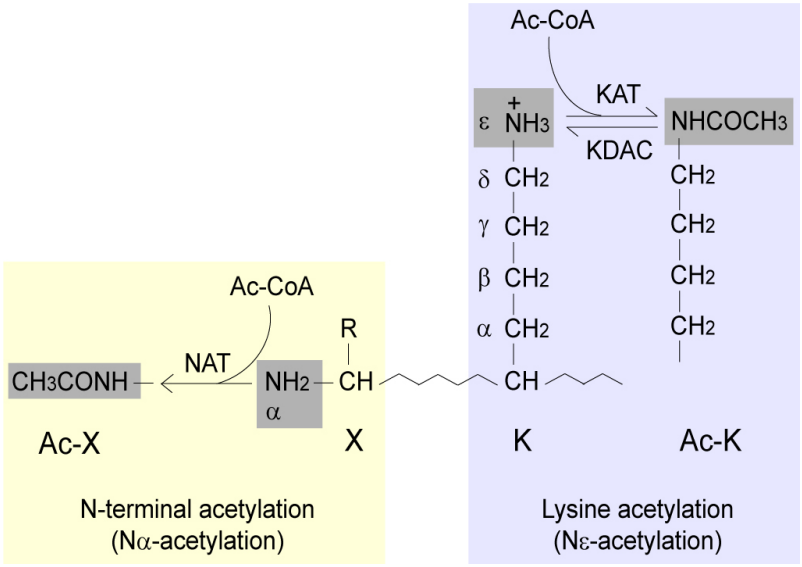

Figure 1.1. Schematic illustration of protein acetylation.

Based on the position of the receptor amino group, protein acetylation is divided into two groups. N-terminal acetylation is catalyzed by N-acetyltransferase (NAT), while lysine acetylation is catalyzed by lysine acetyltransferase (KAT) and removed by lysine deacetylase (KDAC).

1.1.1 Overview: N-terminal acetylation (N^{α}-acetylation)

N-terminal acetylation occurs on the primary amino group of the first amino acid of a polypeptide; therefore it is always at the amino terminus of a protein. This modification is thought to occur cotranslationally in eukaryotes, which is different from most protein modifications. About 50% of yeast proteins and 80% of human proteins are N-terminal acetylated, making it one of the most commonly seen modifications in eukaryotes (Polevoda and Sherman, 2003). Although phenotypic studies suggest that N-terminal acetylation is important for proteins to function properly, little is known about its exact role in regulating protein functions.

N-terminal acetylation is catalyzed by N-acetyltransferases (NATs or NAAs), and no deacetylase has been identified so far. There are five known NAT complexes, NatA-E, and each one has its own substrate sequence preference. Table 1.1 summarizes the components and substrates of these NATs. NatA, NatB and NatC acetylate a wide range of substrates, which, when combined with each other, seems enough to cover most of the N-terminally acetylated proteins in yeast (Polevoda and Sherman, 2003; Starheim et al., 2009). NatA is essential for cell survival and its substrates include proteins regulating transcription, cell cycle progression, apoptosis, etc. NatB has been shown involved in cell proliferation and cell cycle arrest. NatC is important for membrane association of proteins and is required for normal cell growth and survival. NatD was recently found to acetylate histone H2A and H4 in yeast, but its physiological functions remain unclear. NatE is composed of San (see below) and probably NatA components, and no real substrate has been identified so far (Evjenth et al., 2009; Hou et al., 2007).

Table 1.1 Composition and substrates of NAT complexes.

Type	NatA	NatB	NatC	NatD	NatE
Catalytic subunit	Ard1	Nat3	Mak3	Nat4	Nat5 (San)
Auxiliary subunit	Nat1	Mdm20	Mak10 Mak31		Ard1? Nat1?
Substrate preference	Ser- Ala- Gly- Thr- Val- Cys-	Met-Glu- Met-Asp- Met-Asn- Met-Met-	Met-Ile- Met-Leu-Ala-Leu- Met-Leu-Gly-Thr- Met-Trp- Met-Phe-	Ser-Gly-	Met-Leu-Gly-Pro- Met-Leu-Asp-Pro-
Number of yeast substrates	~2000	~1000	~250	2?	?

1.1.2 Overview: lysine acetylation (N^{ε}-acetylation)

Lysine acetylation (N^{ε}-acetylation) occurs posttranslationally on the lysine ε amino group (Fig.2.1). Histones are well known for being acetylated, and a lot more non-histone proteins were later found acetylated due to improvement of the mass spectrometry technique. The lysine side chain is targeted by multiple posttranslational modifications, but those modifications are mutually exclusive on the same lysine. Therefore, lysine is a hot spot where crosstalks between different regulatory pathways happen, and it also plays a major role in the "histone code" theory (Verhey and Gaertig, 2007; Yang and Seto, 2008). Lysine acetylation is now considered a widely used molecular switch ranked similar to phosphorylation. Functional studies revealed that lysine acetylation is critical for various cellular events such as transcriptional regulation and apoptosis (Fig. 1.2), which is achieved by affecting a broad range of protein

properties including stability, subcellular localization, and protein-protein interaction (Spange et al., 2009).

Lysine acetylation is catalyzed by lysine acetyltransferases (KATs) and removed by lysine deacetylases (KDACs). They are often referred to as histone acetyltransferases (HATs) and deacetylases (HDACs) because histones were the first identified lysine-acetylated proteins. KATs are divided into three major groups: Gcn5-related N-acetyltransferases (GNATs), p300/CBP, and MYST proteins. All of them form multi-subunit protein complexes, and their substrate specificity is determined by the regulatory subunits. In addition to histones, other proteins such as p53, FOXO and actin are also acetylated, and many of the KATs responsible for these acetylations remain to be identified (Yang and Seto, 2008). It is noteworthy that the catalytic subunits of some NATs can also acetylate lysines. Ard1 and San, which belong to NatA and NatE respectively, display KAT activity by themselves (Evjenth et al., 2009; Jeong et al., 2002).

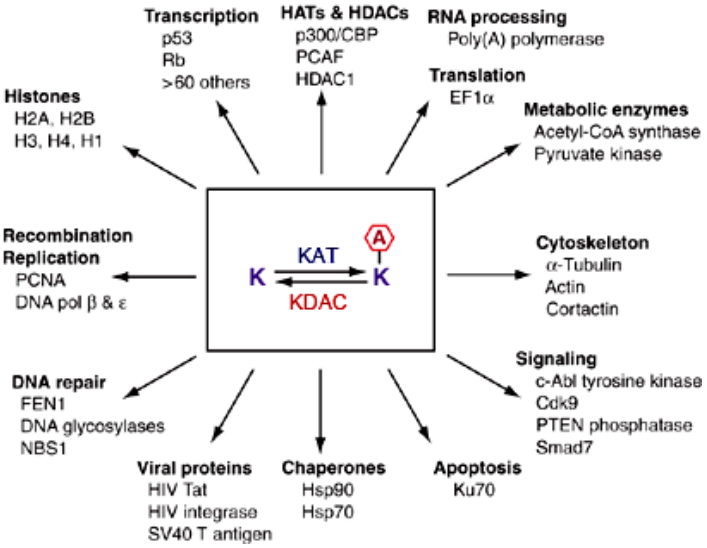

Figure 1.2. Schematic illustration of the cellular functions modulated by lysine (K) acetylation.

(Modified from Yang and Seto, 2007) The red hexagonal containing letter A depicts acetylation. For each cellular function, only representative proteins are shown here.

1.1.3 How lysine acetylation modulates protein functions

As mentioned above, lysine acetylation can alter a wide range of protein properties. One direct consequence is removal of the positive charge, which changes the overall charge of the protein and thus reduces the ionic interaction between the protein and other molecules. For example, histone, the main component of nucleosome, is positively charged at its tail. Hyperacetylation of histone reduces its charge and weakens its ionic interaction with DNA backbone, which is negatively charged. Subsequently, the chromatin is loosened and these loci are now accessible for the transcriptional machinery, leading to increased transcription activity (Brownell and Allis, 1996). Another example is cortactin, which interacts with F-actin via its positively charged region. Hyperacetylation at this region blocks cortactin binding to F-actin and thus reduces cell motility (Zhang et al., 2007b).

In addition to affecting ionic interaction, lysine acetylation also modulates non-ionic protein interactions. The bromodomain protein module binds to acetyl-lysine, and together they establish an acetylation-specific binding partnership similar to that between phospho-tyrosine and SH2 domain. KATs such as P/CAF and CBP bind to acetylated histones and transcription factors via their bromodomains, which results in more acetylations on the neighboring histones or transcription factors and forms a positive feedback loop. Therefore, bromodomain proteins play key roles in regulating gene transcription activity (Yang, 2004).

Lysine acetylation regulates protein stability in multiple ways. It can directly stabilize proteins by competing with ubiquitination, a posttranslational modification also occurring on lysine and targeting proteins for proteasomal degradation. This regulatory

mechanism is commonly utilized by KAT substrates such as p53 and c-Myc (Spange et al., 2009). Interestingly, in the case that acetylation and ubiquitination do not target the same lysine, acetylation can also destabilize proteins by promoting ubiquitination. For example, c-Myc is stabilized by CBP-catalyzed acetylation but destabilized by p300-catalyzed acetylation (Faiola et al., 2005; Vervoorts et al., 2003). In addition to proteasomal degradation, non-proteasomal degradation can also be enhanced by lysine acetylation. The regulation of HNF6 stability by CBP-catalyzed acetylation has been reported (Rausa et al., 2004).

As mentioned above, lysine is targeted by multiple posttranslational modifications. Lysine acetylation thus becomes part of the lysine-based molecular switch for protein functions. In addition to coupling with ubiquitination to regulate protein stability, acetylation forms a binary switch with methylation to regulate protein recruitment. Methylation on histone H3 K9 leads to transcriptional repression and heterochromatin assembly by recruiting HP1, whereas K9 acetylation, usually accompanied by S10 phosphorylation, marks transcriptional activation (Jenuwein and Allis, 2001). Furthermore, acetylation can also couple with sumoylation to regulate protein activity. For instance, two lysine residues on p300 are targeted by both acetylation and sumoylation, which activate and repress the transcriptional activity of p300 respectively. SirT1, a KDAC, represses p300-dependent gene transactivation by deacetylating p300 to allow sumoylation to occur (Bouras et al., 2005). In some cases phosphorylation is also involved in the acetylation/sumoylation switch and adds another layer of regulation. MEF2A contains a phosphorylation-dependent sumoylation motif (PDSM) in which phosphorylation is required for sumoylation to occur. Therefore,

dephosphorylation of this motif leads to loss of sumoylation and promotes acetylation, which then inhibits postsynaptic differentiation (Shalizi et al., 2006).

In addition to coupling with other posttranslational modifications, lysine acetylation by itself can modulate protein activity and in some cases is utilized to regulate KATs and KDACs. For example, p300 acetylates itself to enhance its own acetyltransferase activity and acetylates HDAC1, a KDAC, to abolish the deacetylase activity (Qiu et al., 2006; Thompson et al., 2004). Besides, lysine acetylation also affects protein localization by altering protein-protein interactions. Acetylation of poly (A) polymerase (PAP) by CBP has been shown to block PAP translocation to nucleus by disrupting its interaction with importin complex (Shimazu et al., 2007). Since these two mechanisms are also part of the regulation of KAT activity, they will be further described below.

1.1.4 GNAT superfamily acetyltransferase

Gcn5-related N-acetyltransferases (GNATs) represent a huge protein family in which the members share a structurally conserved catalytic domain termed GNAT acetyltransferase domain. Members of this superfamily are found in all kingdoms of life and mediate diverse functions by modifying a wide range of substrates such as aminoglycoside, serotonin and histones (Vetting et al., 2005). Because many of the substrates are of clinical significance, the enzymological and structural properties of these enzymes have been intensively studied. Structural data revealed that most of the GNAT family members act as dimers or contain two GNAT domains within a single molecule to form a so-called “internal dimer”. In addition to catalyzing the transfer of the acetyl

group, some of the family members also catalyze the transfer of acyl group from acyl-CoA to their substrates. This section will only highlight functions of the acetyltransferases.

GNAT family proteins such as Elp3, Gcn5 and P/CAF catalyze lysine acetylations on histones and have been extensively investigated. Elp3 is the catalytic subunit of the Elongator complex, which plays vital roles in gene transcription, tRNA modification, exocytosis, and neuronal development (Nguyen et al., 2010; Svejstrup, 2007). Gcn5 is the founding member of GNAT superfamily, and studies of Gcn5 established the first link between histone acetylation and transcriptional activation (Brownell and Allis, 1995; Brownell and Allis, 1996). P/CAF acetylates histones as well as many transcription factors including p53, MyoD and TFIIE, hence P/CAF has broad effects on gene transcription (Sterner and Berger, 2000). In addition to Elp3, Gcn5 and P/CAF are also part of multi-subunit protein complexes. In yeast, Gcn5 exists in two distinct protein complexes: the 2 MDa SAGA complex and the 700 kDa ADA complex, and they are conserved throughout the metazoans (Baker and Grant, 2007). Human Gcn5 and P/CAF are both yeast Gcn5 paralogs and form three SAGA-like complexes called STAGA, TFTC, and P/CAF complex. Because they are highly similar to each other, they are sometimes collectively referred to as STAGA (Nagy and Tora, 2007). SAGA is required for viability, and disruption of SAGA in *Drosophila* causes global hypoacetylation of chromatin (Qi et al., 2004). The ATAC complex was originally thought to be the metazoan paralog of the ADA complex, but a recent study revealed more of its components and indicated that it has a similar size to STAGA but has distinct composition and functions (Wang et al., 2008). Another GNAT family acetyltransferase

Atac2 were later shown to be a core component of ATAC, and disruption of Atac2 gene in mice results in embryonic lethality due to deregulated apoptosis and cell cycle progression (Guelman et al., 2009).

In addition to lysine residues within proteins, amino groups on natural compounds are also targets of GNAT family members. Aminoglycoside N-acetyltransferase (AgNATs), the first identified GNAT family member, acetylates aminoglycosides with antibiotic properties such as gentamicin and kanamycin (Davies and Wright, 1997). Acetylated antibiotics have less binding affinity to their targets, and thus bacteria expressing AgNATs exhibit increased resistance to those antibiotics (Llano-Sotelo et al., 2002). Moreover, serotonin N-acetyltransferase (SNAT, or arylalkylamine N-acetyltransferase, AANAT) acetylates serotonin to synthesize melatonin, a hormone involved in circadian rhythms and human moods. Unlike most GNAT family members, SNAT works as a monomer (Hickman et al., 1999). Another example is glucosamine-6-phosphate N-acetyltransferase (GNA1), which acetylates glucosamine-6-phosphate to synthesize UDP–*N*-acetylglucosamine and is essential for budding yeast to grow (Mio et al., 1999).

1.1.5 Regulation of the activity of GNAT superfamily acetyltransferase

Given that lysine acetylation is an important regulatory protein modification, the activity of KAT needs to be tightly controlled. Several mechanisms are utilized to regulate the enzymatic activity of KAT, including posttranslational modifications, protein-protein interactions, changes of subcellular localization, and protein stability

(Mellert and McMahon, 2009). This section will focus on the regulatory machineries of GNAT superfamily acetyltransferases, most of which are also shared by other KATs.

Autoacetylation seems to be a fundamental mechanism to regulate KAT activity, given that KATs from all three major families have been shown catalyzing autoacetylation (Mellert and McMahon, 2009). P/CAF catalyzes both intermolecular and intramolecular autoacetylation (Santos-Rosa et al., 2003). The intramolecular autoacetylation targets five lysine residues within its nuclear localization signal. This autoacetylation modulates P/CAF functions in two ways. One is to stimulate its own enzymatic activity, and this autonomous feed-forward mechanism is very similar to the regulation of kinase activity by autophosphorylation. The other is to facilitate translocation of P/CAF from cytoplasm to nucleus, supported by the finding that non-autoacetylated P/CAF accumulates in the cytoplasm (Blanco-Garcia et al., 2009).

In addition to autoacetylation, other posttranslational modifications also contribute to the regulation of KAT activity. For example, the activity of human Gcn5 is inhibited by phosphorylation catalyzed by the DNA-dependent protein kinase (DNA-PK) holoenzyme (Barlev *et al.*, 1998). Moreover, the acetylation/sumoylation switch is also involved in regulating KAT activity. While regulation of p300 activity by this switch is well-characterized (see above), more work is required to dissect the effect of sumoylation on Gcn5 (Sterner et al., 2006)

As mentioned above, GNAT family proteins are part of multi-subunit protein complexes, and their substrate specificity is determined by the regulatory subunits within the complex. For example, human Gcn5 by itself preferentially acetylates histone H3 K14. However, when associated with STAGA, its target expands to H3 K9, K18 and K23 as

well as H2B and H4 (Nagy and Tora, 2007). When associated with ATAC, Gcn5 acetylates only H3 K9 (Guelman et al., 2009; Wang et al., 2008). Human Atac2 alone shows only weak KAT activity targeting histone H4, but disruption of ATAC by deleting the Atac2 gene results in significant decrease of acetylation on histone H4 K5, K12 and K16 (Guelman et al., 2009). Therefore, the regulatory subunits of these complexes are crucial for directing the KATs to different target sites or even different substrates to perform distinct functions.

1.1.6 San

San (separation anxiety), also known as Nat5, Nat13 or Naa50, is a 169 amino acid long cytosolic protein belonging to GNAT superfamily. It was first described as a member of a putative NAT family based on the sequence similarity to yeast Nat5 (yNat5) (Polevoda and Sherman, 2003). San has been found associated with NatA complex, which may help stabilizing San (Hou et al., 2007). Nevertheless, depletion of NatA components did not phenocopy depletion of San, suggesting that San acts independent of NatA (Hou et al., 2007). In addition, San is dispensable for NatA functions (Gautschi et al., 2003). Together these findings indicate that San performs functions distinct from those of NatA, therefore San is now categorized into a new NAT family called NatE (Starheim et al., 2009).

Although San was predicted as a NAT, its NAT activity was not validated until recently (Evjenth et al., 2009). Even though the substrate specificity has been established in vitro, the in vivo substrate of San remains unknown. As a result, whether San is a physiologically relevant NAT needs to be further investigated. Nevertheless, similar to

Ard1 (see above), San catalyzes both N-terminal and lysine acetylation. Histone H4 and San itself have been shown acetylated on lysines by San in vitro (Evjenth et al., 2009; Hou et al., 2007). San catalyzes intramolecular autoacetylations on lysine 34, 37 and 140, which, unlike those on other KATs, reduce its KAT activity and simultaneously enhance its NAT activity. Therefore, autoacetylation of San serves as a molecular switch regulating its NAT and KAT activity. In addition to acetylation, San was also found being phosphorylated on threonine 12 and tyrosine 110 in vivo (Choudhary et al., 2009; Dephoure et al., 2008; Rush et al., 2005). The biological significance of these phosphorylations remains to be dissected.

San is required for mitotic centromeric cohesion in *Drosophila* and human cells (Hou et al., 2007; Williams et al., 2003). Upon San depletion, cohesin was no longer localized to the centromere in metaphase cells. The enzymatic activity of San is necessary for this function, but whether it acts through its NAT or KAT activity remains obscure. A recent study in *Drosophila* further demonstrated that San also contributes to chromosome resolution while its function in centromeric cohesion is dispensable in germ line cells (Pimenta-Marques et al., 2008). Given that San plays important roles in chromosome dynamics, it is tempting to speculate that histone H4, which has been shown acetylated by San in vitro, may be the downstream effector of San for these events. Further studies are required to test this hypothesis. Interestingly, these functions of San are conserved only within higher eukaryotes, because deleting yNat5 did not cause any similar defect (Gautschi et al., 2003). This is consistent with the fact that San is well conserved among higher eukaryotes (>70% sequence identity) but only shows 25% sequence identity with

yNat5 (Arnesen et al., 2006). It is possible that San gained important functions at certain point during evolution.

1.2 Microtubules

1.2.1 Overview: Microtubule (MT) functions

Microtubules (MTs) are one of the three major components of the cytoskeleton. In addition to supporting the mechanical integrity of the cell, MTs serve as tracks for the transport of vesicles and organelles. Motor proteins such as dynein and kinesin carry their cargos and move along MTs (Caviston and Holzbaur, 2006). By facilitating vesicle transport, MTs organize the cellular compartments and establish cell shape and polarity. In interphase cells, MTs can form motile structures such as flagella and cilia; in mitotic cells, MTs reorganize to form the bipolar spindle and segregate chromosomes into daughter cells.

MTs are composed of α/β tubulin heterodimers, which assemble head-to-tail into protofilaments and then adhere laterally to form polar hollow tubes. Polarity of MTs gives rise to the different polymerization rates of the two ends, with the plus end (β-tubulin) assembling faster than the minus end (α-tubulin) (Fig. 1.3A). In the cell, MTs mostly emerge from the centrosome (generally referred to as MTOC), with their minus ends attached to the matrix of the centrosome and plus ends growing toward the cell periphery (Fig. 1.3B). γ-tubulin, another member of the tubulin family, forms ring complexes at the centrosome and plays key roles in nucleating MTs (Raynaud-Messina and Merdes, 2007). MTs are intrinsically unstable and the plus end exhibits a behavior

called dynamic instability, characterized by stochastic transitions between growing and shrinking phases (Fig. 1.3A) (Mitchison and Kirschner, 1984). The transition from growth to shrinkage is called catastrophe and the opposite transition is called rescue. Dynamic instability allows MTs to search for binding partners involved in cell architecture, a model known as "search and capture"(Kirschner and Mitchison, 1986). Once the stabilizing cues are captured, the MTs are stabilized and strong enough to conduct pulling force to target organelles. Cell migration and mitotic chromosome segregation are good examples, in which the stabilizing cues are located at the plasma membrane and the kinetochores, respectively (Fig. 1.3B).

1.2.2 MT assembly and disassembly

α- and β-tubulins are highly conserved among species, and they are very similar in terms of size and structure (Nogales, 2001). Both α- and β-tubulin bind to a GTP molecule and they form a heterodimer with the α-tubulin-bound GTP buried within the dimer (Fig. 1.3A). Therefore, only the β-tubulin-bound GTP is hydrolysable and exchangeable. Upon polymerization, the β-tubulin-bound GTP is hydrolyzed and becomes non-exchangeable due to its contact with the adjacent α-tubulin. Therefore, MTs are mainly made of GDP-tubulins except for the plus end, which is capped by GTP-tubulins (Fig. 1.3A) (Dimitrov et al., 2008; Mitchison and Kirschner, 1984). Loss of the GTP cap leads to MT catastrophe, and depolymerized GDP-tubulins can be recycled for further polymerization following the exchange of GDP for GTP. Interestingly, MTs assemble in the presence of GMPCPP, a slowly hydrolysable GTP analog (Hyman et al.,

1992), and GTP-tubulins have been detected in the MT body (Dimitrov et al., 2008), suggesting that GTP hydrolysis is not required for MT assembly. GMPCPP-incorporated MTs are more stable than normal GDP-MTs, indicating that GDP-tubulins contribute to MT disassembly. Consistent with this idea, the GTP-tubulin remnants in the MT body coincide with the position where rescue events initiate (Dimitrov et al., 2008).

The different effects of GDP-tubulin and GTP-tubulin on MT disassembly are caused by their different conformations (Nogales and Wang, 2006). At the growing MT plus end, protofilaments form open sheets and sequentially close into cylinders (Chretien et al., 1995). Upon MT disassembly, protofilaments peel off from the plus end and form ring-like structures (Fig. 1.3A) (Mandelkow et al., 1991). These were the first hints for the possibility that GTP-tubulin and GDP-tubulin adopt different conformations and in turn affect protofilament curvature. The x-ray structure of tubulin in a zinc-induced tubulin sheet is in a straight conformation (Lowe et al., 2001; Nogales et al., 1998). Because the zinc sheet is composed of straight protofilaments bound to the stabilizer taxol, it is thought to structurally resemble MTs (Nogales et al., 1999). On the other hand, tubulin has been shown in a curved conformation when associated with a stathmin-like domain (Gigant et al., 2000). This represents the tubulin structure in the depolymerized state, and the curvature is due to intradimer and interdimer kinks. Cryo-electron microscopy revealed that GDP-tubulin protofilaments are more curved than GMPCPP-tubulin protofilaments (Muller-Reichert et al., 1998), and further investigation demonstrated that the intradimer bend (containing GTP) is indeed smaller than the interdimer bend (containing GDP) (Wang and Nogales, 2005), supporting the model that GTP-tubulin is in a straighter conformation than GDP-tubulin.

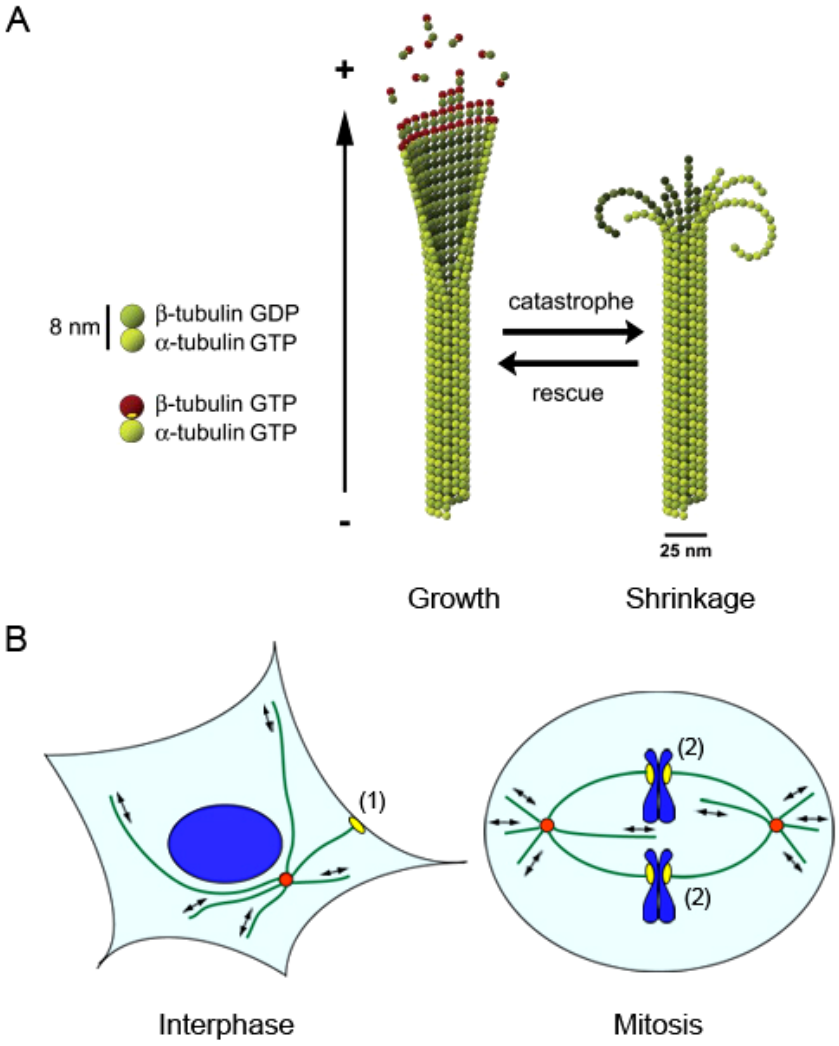

Figure 1.3. Dynamic instability of microtubules (MTs).

A. (Modified from Pastugllia and Bouchez, 2007) MT, a polymer of tubulin heterodimer, is a polar tube of 25 nm in diameter. The end where β-tubulin is exposed is termed the plus end (+) because it grows faster. MT assembly starts from an open sheet of tubulin protofilaments, which then close to form a cylinder. Upon disassembly, protofilaments peel off from the plus end. The plus end exhibits dynamic instability, characterized by stochastic shifts between growth and shrinkage. The transition from growth to shrinkage is called catastrophe, and the reverse process is called rescue. **B.** In cells, MTs (green) emanate from the centrosomes (orange) with their plus ends extending freely and highly dynamic (double-headed arrows). MTs become stable when the plus ends are captured by the stabilizing cues (yellow), which may localize at the plasma membrane (1) or chromosomes (blue) (2) during mitosis.

Together the above studies support the following model describing the molecular mechanism of the dynamic instability (Fig. 1.4). GDP-tubulin is intrinsically curved and is partially straightened by GTP exchange. The conformation of GTP-tubulin is straight enough to provide lateral contacts between protofilaments and is capable of forming the open sheet structure observed at the growing plus end. Closure of the tubulin sheet into a cylinder induces GTP hydrolysis, and those tubulin dimers are straightened by lateral constrains from the tubulin lattice, resulting in a fully straight MT (Rice et al., 2008). This model also explains the observation that there is no energy release during MT assembly (Caplow et al., 1994). All the energy from GTP hydrolysis is converted to structural constrains by inducing the conformational changes of tubulin dimers. The energy is restricted in the MT body by the GTP-tubulin cap, and loss of the cap allows the GDP-tubulins to adopt their original curved structure and in turn results in catastrophe and energy release, which may be used to drive the movement of protein complexes such as the Ndc80/Dam1 complex (Tanaka and Desai, 2008).

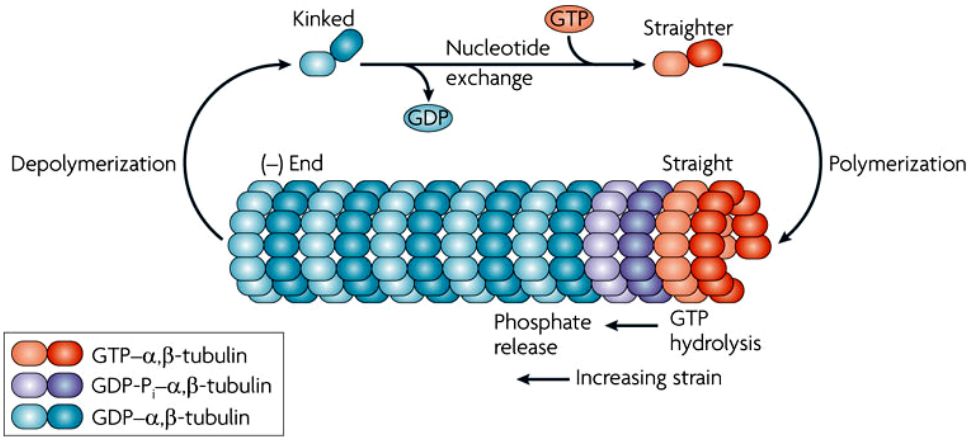

Figure 1.4. GTP cycle of tubulin.

(Adapted from Howard and Hyman, 2009) GDP-tubulin is intrinsically kinked. Exchange of GDP for GTP partially straightens tubulin and allows tubulin to undergo polymerization. Polymerized tubulin becomes fully straight due to lateral constrains within the MT. Polymerization induces GTP hydrolysis and in turn increases the strains within the GDP-tubulin lattice. These strains drive MT depolymerization, releasing energy and free GDP-tubulins.

1.2.3 The MT poisons

Given that MT dynamics are essential for faithful chromosome segregation during mitosis, tubulin has been a highlighted target for anti-mitotic drugs, which have been applied for cancer therapy. To date four major classes of tubulin-binding agents have been identified: colchicine analogs, vinca alkaloids, taxoids and pelorusides, distinguished by their different binding sites on the tubulin dimer. As MT destabilizing agents, colchicine analogs (colchicine) and vinca alkaloids (vinblastine) bind to intra-dimer and inter-dimer regions respectively, both of which abolish the protofilament straightening by increasing the curvatures (Gigant et al., 2005; Ravelli et al., 2004). Nocodazole, another MT destabilizing drug preferred by researchers, reversibly binds to

tubulin at the same pocket as colchicine does despite of their different structures (Hoebeke et al., 1976). Taxoids (taxol) bind to the luminal side of β-tubulin, which locks tubulin dimer in the straight conformation and thus stabilizes MTs (Elie-Caille et al., 2007; Nogales et al., 1998). Pelorusides (peloruside A) are categorized as a new class of MT stabilizing drug because they are effective on taxol-resistant tumor cells (Gaitanos et al., 2004). However, the binding site of peloruside A on tubulin remains contradictory (Huzil et al., 2008; Jimenez-Barbero et al., 2006).

1.2.4 Regulation of MT length: MT polymerase/depolymerase and severing enzymes

Given the stochastic nature of the MT dynamics, it is crucial to balance the growth and shrinkage of MTs to achieve the optimal length and numbers for different cellular functions. In cells there are numerous MT-associated proteins (MAPs) regulating MT properties and functions, and those MAPs contributing to the modulation of MT dynamics are summarized in Fig. 1.5 (Wade, 2009). This section will focus on the regulators of MT length: MT polymerases/depolymerases as well as MT severing enzymes.

MT polymerases/depolymerases directly accelerate the speed of MT assembly or disassembly to cause net growth or shrinkage (Fig. 1.5). The best-known MT polymerase is XMAP215, a long thin protein with multiple tubulin binding domains (TOG domains) (Cassimeris et al., 2001). Localized at MT plus ends, XMAP215 binds to a tubulin dimer and sequentially adds tubulin to the growing end by stabilizing the structural intermediate (Brouhard et al., 2008). This reaction does not require energy input; therefore it can be reversed when the concentration of free tubulin is low (Brouhard et al., 2008; Shirasu-

Hiza et al., 2003). In other words, XMAP215 actually acts as a catalyst, which accelerates the reaction in both directions by stabilizing the transition intermediate.

MCAK, a member of the kinesin-13 family, is an ATP-dependent MT depolymerase, which promotes catastrophe by binding to and bending the protofilaments at both ends (Hertzer and Walczak, 2008). Unlike other kinesins, MCAK does not move directionally along MTs; instead it passively diffuses along MTs and finally reaches the end, a mechanism known as "diffuse and capture" (Helenius et al., 2006). The energy from ATP hydrolysis is used to remove tubulin dimers from the protofilaments (Hunter et al., 2003).

Kip3, which belongs to the kinesin-8 family, is another kinesin showing MT depolymerase activity, but only at the plus end (Gupta et al., 2006; Varga et al., 2006). Kip3 depolymerizes MT in a way similar to MCAK, but it differs from MCAK by coupling ATP hydrolysis to the movement along MTs toward the plus end. Another feature of the Kip3-mediated MT depolymerization is its dependency on MT length—the longer the MT the faster Kip3 will depolymerize it. This can be explained by the high processivity of Kip3, which has an average 12 μm long "step" (Varga et al., 2006). Since almost every MT-bound Kip3 can reach the plus end, the longer the MT the more Kip3 will accumulate at the plus end and the higher the depolymerization rate will be. Such length-dependent activity may be important to maintain MTs in a certain length, like those in the mitotic spindle (Goshima et al., 2005).

Another mechanism of adjusting MT length is to cut MTs in the middle, a process known as MT severing. MT severing is critical for the construction of the mitotic spindle, non-centrosomal MT array, and the regulation of flagella length (Casanova et al.,

2009; Roll-Mecak and Vale, 2006; Zhang et al., 2007a). Katanin, spastin, and fidgetin have been identified as MT-severing enzymes, and they are AAA proteins closely related to each other (Frickey and Lupas, 2004). The katanin, the best-characterized one, is a heterodimer composed of a p60 catalytic subunit and a p80 regulatory subunit. Katanin p60 subunit is thought to form hexamers in the presence of ATP and MTs (McNally, 2000), and small-angle x-ray scattering studies revealed that ATP-bound spastins form a ring-shaped hexamer (Roll-Mecak and Vale, 2008). The hexamer is proposed to dock on the surface of MT, with the tubulin C-terminus threading through the central pore. ATP hydrolysis may locally destabilize the MT lattice by inducing conformational changes and in turn lead to MT breakage.

1.2.5 Regulation of MT stability: MT-stabilizing/destabilizing proteins

In addition to length, stability is another important property of MTs being affected by dynamic instability (Fig. 1.5). As mentioned above, stable MTs are required for driving the movement of chromosomes during mitosis, and it is crucial to keep MT stable enough for vesicle trafficking inside the cell, especially in neuronal cells. MT stability can be regulated by tuning the balance between catastrophe and rescue, and stable MTs tend to undergo rescue instead of catastrophe. MAPs contributing to MT stability control are called MT stabilizing/ destabilizing proteins and will be highlighted in this section.

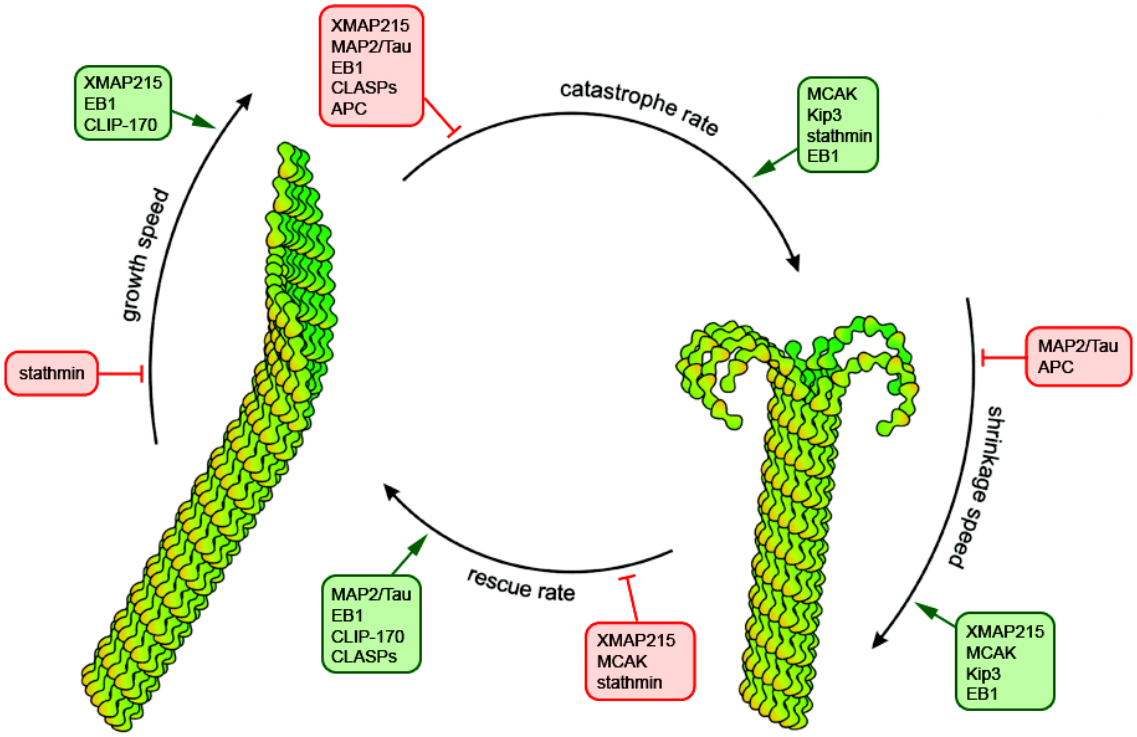

Figure 1.5. Schematic illustration of MAPs regulating MT dynamics.

(Modified from van der Vaart *et al.*, 2009) MT dynamics is determined by both the growth/shrinkage speed and the catastrophe/rescue rate. MAPs that play positive roles in a process are listed in green boxes with a green arrow pointing to the regulated process. MAPs that play negative roles are listed in red boxes.

MAP2, MAP4, and Tau belong to the MAP2/Tau family, and their MT-stabilizing activities have been well-characterized (Dehmelt and Halpain, 2005). MAP4 is expressed in non-neuronal tissues, while MAP2 and Tau are found in neurons and play important roles in neuronal differentiation. All three proteins contain 3 to 5 MT-binding repeats at their C-termini, and phosphorylation at a KXGS motif within the repeat abolishes its binding to MTs. MAP2/Tau family members bind longitudinally along MTs and stabilize them by inhibiting catastrophe and MT severing activity (Al-Bassam et al.,

2002; Gamblin et al., 1996; McNally et al., 2002). Moreover, patches of Tau on MTs inhibit the motility of kinesin-1 and dynein (Dixit et al., 2008), making Tau the "road block" for the MT-dependent transport.

Op18/stathmin was initially identified as an onco-protein and later recognized as a key MT-destabilizing protein. Structural analysis showed that stathmin is a rod-shaped molecule and can bind two tubulin dimers to form a curved complex (Gigant et al., 2000; Steinmetz et al., 2000). Two mechanisms were proposed regarding how stathmin destabilizes MTs. One is to bind to MT ends and promote catastrophe (Belmont and Mitchison, 1996), and the other is to sequester free tubulin dimers from being incorporated into MTs (Curmi et al., 1997; Jourdain et al., 1997). It has been demonstrated that both activities exist and can be uncoupled due to their different needs of stathmin: the former requires the N-terminal part of stathmin while the latter requires the C-terminal part (Howell et al., 1999). However, the mechanism by which stathmin promotes catastrophe is still under debate (Cassimeris, 2002). The abilities to destabilize MTs and inhibit centrosomal nucleation of MTs make stathmin one of the major regulators of MT polymer mass in vivo (Holmfeldt et al., 2009; Ringhoff and Cassimeris, 2009). Phosphorylation prevents stathmin from binding to tubulins, which is important to regulate MT organization during mitosis, cell migration, and T-cell signaling (Holmfeldt et al., 2009).

1.2.6 MT plus-end tracking proteins (+TIPs)

+TIPs such as XMAP215, MCAK, end-binding (EB) proteins and CLIP-170 accumulate at the MT plus ends and locally regulate MT dynamics as well as attachments

to cortical structures (Fig. 1.5) (Akhmanova and Steinmetz, 2008). These MT-to-cortex attachments are critical for directional transport, force generation, signal transduction, and subsequent polarity establishment (Siegrist and Doe, 2007). This section will mainly focus on EB1, the key player at the plus end.

EB family members preferentially bind to the open sheet structure at the plus end, which allow them to track the plus end autonomously (Bieling et al., 2007; Sandblad et al., 2006). EB1 has been shown to accelerate MT growth by facilitating nucleation and sheet closure, and it can increase the rescue frequency by enhancing the lateral contacts between protofilaments. However, at a lower concentration EB1 also promotes catastrophe possibly due to shortened open sheet (Vitre et al., 2008). Given that EB1 prevents catastrophe in vivo, it has been proposed that the local concentration of active EB1 is tightly controlled, possibly through competition between +TIPs for binding sites at the plus end (Komarova et al., 2009).

In addition to directly affecting MT dynamics, EB1 loads other +TIPs to the plus end. CLIP-170, which binds to tubulin via its CAP-Gly domains (cytoskeleton-associated protein glycine-rich), requires EB1 to be loaded onto the plus end (Bieling et al., 2008; Dixit et al., 2009). CLIP-170 also serves as a promoter for MT nucleation and rescue (Arnal et al., 2004; Komarova et al., 2002). Other +TIPs such as MCAK, CLASPs, and APC bind to EB1 via their SxIP motif (Honnappa et al., 2009). Similar to the MAP2/Tau family, CLASPs and APC stabilize MTs by preventing catastrophe and promoting rescue (Kita et al., 2006; Mimori-Kiyosue et al., 2005), but their effects are more restricted to the plus end due to their association to EB1.

1.2.7 Tubulin isotypes and posttranslational modifications

In addition to associating with different MAPs, MTs can be intrinsically diversified by incorporating different tubulin isotypes or tubulins carrying different post-translational modifications. This diversity not only affects MT stability by itself but also affects MT functions by recruiting different MAPs.

Tubulin isotypes are well conserved across vertebrates. Table 1.2 summarizes the 7 α-tubulins and 8 β-tubulins found in vertebrates. The main difference comes from the C-terminal tail (CTT, the last 15-20 amoni acids), which lies on the MT surface and is essential for MAP recruitment. Although these isotypes have their own tissue-specific expression patterns, some of them are functionally interchangeable; hence their physiological significance remains elusive (Luduena, 1998). However, in *C. elegans* there is evidence indicating that a particular set of tubulin heterodimer increases the number of protofilament within a MT from 11 to 15, suggesting that tubulin isotypes composition can regulate MT functions (Fukushige et al., 1999). Furthermore, tubulin isotype composition affects MT stability in vitro (Schwarz et al., 1998), and it has been shown that the sensitivity of cancer cells to anti-mitotic drugs correlates with their β-tubulin isotype expression profiles. High-level expression of β_{III}-tubulin, which is normally expressed in neuronal cells and testicular Sertoli cells, has been shown associated with the resistance to taxol or vinca alkaloids in a wide range of cancer types (Seve and Dumontet, 2008). In addition to increasing MT dynamics, β_{III}-tubulin also inhibits DNA damage-induced apoptosis, leading to the resistance to several DNA-

damaging agents in those β_{III}-tubulin-overexpressing cancer cells. Therefore β_{III}-tubulin is thought to be a survival-promoting factor against cellular stress (Kavallaris, 2010).

Table 1.2 Vertebrate tubulin isotypes

Tubulin isotype	C-terminal sequence	Expression profile
αI	VDSVEGEEEGEEY VDSVEGEGEEEGEEY	Ubiquitous
αII	VDSVEAEAEEGEEY	Testis
αIII	IDSYEDEDEGEE	Brain, muscle
αIV	ADSADGEDEGEEY	Blood
αV	TDSFEEENEGEEF	Heart, skeletal muscle, testis
αVI	MGSVEAEGEEEDRDTSC	Testis
αVII	TESGDGGEDEEDEY	Ovary
βI	YQDATAEEEEDFGEEAEEEA	Ubiquitous
βII	YQDATADEQGEFEEEEGEDEA	Brain, muscle
βIII	YQDATAEEEGEMYEDDEEESEAQGPK	Neurons, Sertoli cells
βIVa	YQDATAEQGEFEEEAEEEVA	Brain
βIVb	YQDATAEEEGEFEEEAEEEVA	Ubiquitous
βV	YQDATANDGEEAFEDEEEEIDG YQDATVNDGEEAFEDEDEEEINE	Ubiquitous but in a low level
βVI	FQDAKAVLEEDEEVTEEAEMEPEDKGH FQDVRAGLEDSEEDAEEAEVEAEDKDH	Hematopoietic tissues
βVII	YQDATAEGEGV	Brain?

Table 1.3 Posttranslational modifications of tubulin

Modification	Description	Forward enzyme	Reverse enzyme	Comment
Lysine acetylation	Addition of acetyl group on lysines	The Elongator complex	HDAC6, SirT2	α-tubulin lysine 40 is best characterized
Phosphorylation	Addition of phosphate	Cdk1, Syk, PSK, Fes	?	β-tubulin serine 172 is best characterized
Polyglutamylation	Addition of glutamates as a side chain	TTLL family	?	Variable side chain length
Polyglycylation	Addition of glycines as a side chain	TTLL family	?	Variable side chain length
Detyrosination	Removal of C-terminal tyrosine	Nna1/CCP1?	TTL family	α-tubulin only
Δ2	Removal of penultimate glutamate from detyrosinated α-tubulin	?	Irreversible	α-tubulin only

Tubulins are targeted by multiple posttranslational modifications, which are thought to codify diverse tubulin functions. This is conceptually parallel to the histone code hypothesis and thus called the tubulin code hypothesis (Verhey and Gaertig, 2007). Table 1.3 summarizes those modifications and the involved enzymes. In most cases, tubulin modifications are enriched at the CTTs and occur on tubulins incorporated into MTs instead of free tubulins. One exception is the phosphorylation of β-tubulin on S172,

which occurs on free tubulins during mitosis and prevents modified tubulins from being incorporated into MTs. The phosphorylation is catalyzed by Cdk1 and may affect GTP binding and exchange of β-tubulin (Fourest-Lieuvin et al., 2006). Several other phosphorylations and enzymes catalyzing them have been reported, but their physiological significances remain unclear (Verhey and Gaertig, 2007). Interestingly, phosphorylation, which is commonly observed on other proteins, seems to be a minor modification for tubulins. Given that tubulin is highly negatively charged, introducing another negatively charged phosphate group may not affect tubulin structure or net charge as dramatically as those seen on other proteins (Westermann and Weber, 2003).

The best-described tubulin acetylation is on α-tubulin K40, and several other acetylation events have been reported in a proteomics study (Choudhary et al., 2009; LeDizet and Piperno, 1987). K40 acetylation, which mostly occurs on stable MTs, is catalyzed by the Elongator complex and is removed by HDAC6 and SirT2 (Creppe et al., 2009; Hubbert et al., 2002; North et al., 2003; Solinger et al., 2010). Whether K40 acetylation regulates MT dynamics or stability is still under debate, with each side supported by multiple observations. It has been shown that K40 acetylation has no effect on MT dynamics in vitro or MT stability in vivo (Maruta et al., 1986; Palazzo et al., 2003). However, studies focusing on HDAC6 suggest that K40 acetylation stabilizes MTs and decreases MT dynamics (Matsuyama et al., 2002; Tran et al., 2007). The recent finding that K40 acetylation may regulate MT stability by modulating α-tubulin turnover adds even more complexity (Solinger et al., 2010). The controversy may be caused in part by manipulation of the K40 acetyltransferases/ deacetylases, which have other substrates in addition to tubulin. Although non-essential for cell survival, K40 acetylation

has been shown involved in motor-driven vesicle transport (Dompierre et al., 2007; Kawaguchi et al., 2003; Reed et al., 2006), cell motility (Hubbert et al., 2002), and neuronal development (Creppe et al., 2009; Solinger et al., 2010). Given that K40 locates at the MT luminal side, it remains to be determined how K40 acetylation affects motor protein movement on the surface of MTs. There may be some allosteric changes of MT structure upon K40 acetylation.

Most α-tubulin isotypes contain a tyrosine at their C termini. Removal of the tyrosine by Nna1/CCP1 metallocarboxypeptidase is called detyrosination, which occurs on MTs and accumulates over time (Gundersen et al., 1987; Kalinina et al., 2007). After MT disassembly, tubulin tyrosine ligase (TTL) is responsible for adding tyrosine back to those detyrosinated tubulins (Ersfeld et al., 1993). The two processes together form the tyrosination/detyrosination cycle. Removing the C-terminal glutamic acid of detyrosinated tubulin by deglutamylation generates Δ2-tubulin, which is no longer a TTL substrate and thus escapes the cycle (Paturle-Lafanechere et al., 1991; Rudiger et al., 1994). Instead of affecting MT dynamics, tyrosination and detyrosination are implicated in regulating the association between MTs and MAPs. Since detyrosination occurs after MT assembly, tyrosinated tubulin is enriched at the plus end while the MT body contains detyrosinated tubulins. Kinesin-1 has been shown preferentially binding to and moving on detyrosinated tubulin (Dunn et al., 2008; Kreitzer et al., 1999). The importance of tubulin tyrosination in neuronal development was revealed by the analysis of TTL null mice, which die perinatally due to neuronal disorganization in their brains (Erck et al., 2005). The phenotypes may be caused by mislocalization of CLIP-170, which localizes to

the plus end by binding to tyrosinated tubulins via its CAP-Gly domains (Erck et al., 2005; Mishima et al., 2007).

Polyglutamylation, in which a polyglutamate side chain of varying length is attached to one or more glutamic acids within the CTT, can occur on both α- and β-tubulin (Edde et al., 1990; Redeker et al., 1991; Redeker et al., 1992). Polyglutamylation is enriched on stable MT-based structures such as centrioles, primary cilia, the mitotic spindle, and the midbody (Bobinnec et al., 1998). It is also prominent on axonal MTs in neuronal cells (Audebert et al., 1993). Polyglutamylation is catalyzed by TTL-like (TTLL) glutamylases, a big protein family in which most members have their own specificity in terms of substrate and catalytic activity (Fukushima et al., 2009; Janke et al., 2005). Similar to detyrosination, polyglutamylation accumulates over time, and it regulates MAP binding to MT rather than MT dynamics. It has been shown that Tau preferentially binds to polyglutamylated tubulin, especially one with a chain of three glutamyl units (Boucher et al., 1994). Analysis of the ROSA22 mutant mice lacking polyglutamylated α-tubulin revealed that MAP1A and multiple kinesins have lower binding affinity to MTs. Consequently, the mislocalization of KIF1A in neurons leads to impaired synaptical transmission (Ikegami et al., 2007). In addition, polyglutamylation accumulates during cilia assembly and peaks earlier than detyrosination or acetylation, suggesting that it may contribute to cilia assembly by facilitating intraflagellar transport (Sharma et al., 2007).

Similar to polyglutamylation, polyglycylation is caused by addition of polyglycine side chains to one or more glutamic acids within the CTT of both α- and β-tubulin (Redeker et al., 1994; Redeker et al., 2005). Nevertheless, polyglycylation has a

more restricted distribution within the cell: it is enriched mostly on axonemes of motile cilia and flagella (Bre et al., 1996). Polyglycylation is also catalyzed by TTLL family proteins. During cilia maturation, the length of the glycyl chain increases, which in turn facilitates ciliary motility (Bre et al., 1996; Sharma et al., 2007). However, given that primary cilia also contain polyglycylated tubulins, tubulin glycylation may generally contribute to axoneme maturation or maintenance (Davenport et al., 2007). In ciliates such as *Tetrahymena*, lack of β-tubulin glycylation is lethal and can be partially rescued by restoring some of the glycylation, suggesting that certain level of tubulin glycylation is essential for cell survival (Xia et al., 2000).

In conclusion, tubulin modifications regulate MT functions by affecting MT properties as well as modulating the association of MAPs with MTs. However, many of the enzymes involved in these modifications remain elusive, and a lot of novel modifications revealed by proteomic studies have not been explored yet. Further investigation is required to identify those unknown enzymes as well as to elucidate the biological significance of the novel modifications, which will lead to better understanding about how tubulin modifications modulate MT functions and how these processes are regulated.

1.3 Summary of the dissertation

San is necessary for proper sister chromatid cohesion and chromosome resolution, but little is known about the mechanism by which San performs its function or San activity is regulated. I sought to identify the downstream effector and upstream regulator

of San, and by affinity purification I found that tubulin is a San substrate. San acetylates free tubulin heterodimer but not taxol-stabilized MT, and the target site was mapped on β-tubulin lysine 252 by both mass spectrometry and site-directed mutagenesis. The acetylation-mimicking tubulin mutants were incorporated into the MT cytoskeleton in HeLa cells and gave no obvious MT defect. However, after cold-induced MT catastrophe, the mutants were incorporated into regrowing MTs in a much slower rate, and the MT regrowth was accelerated in San-depleted cells. Together these findings suggest that San negatively regulates MT assembly by acetylating β-tubulin lysine 252 and impeding the incorporation of acetylated tubulin.

In addition, during the process of looking for San substrates, I found that the soluble protein fraction of HeLa cell lysate reduced the level of autoacetylation of San. The level of pre-catalyzed autoacetylation of San did not decrease over time when incubated with the fraction, suggesting that the reduction is due to inhibition of San activity rather than deacetylation of San. I further demonstrated that this inhibitory effect is protein-based and ATP-dependent, but ATP hydrolysis is not required. The San inhibitor was partially purified by ammonium sulfate fractionation and ATP-conjugated resin, but the identity of the protein remains to be elucidated. Moreover, after the gel filtration chromatography, the activity of San inhibitor was restored only when multiple fractions were combined, suggesting that the San inhibitor may exist as a multi-subunit protein complex.

CHAPTER TWO

SAN DOWN-REGULATES MT ASSEMBLY BY ACETYLATING BETA-TUBULIN AND IMPEDING TUBULIN POLYMERIZATION

2.1 Introduction

Tubulin, the building block of MT (MT), is regulated by various MT-associated proteins and posttranslational modifications (Westermann and Weber, 2003). These modifications are crucial for fine-tuning the property of tubulin and MTs to suit their diverse functions. Tubulin acetylation was first documented in 1981 and the best characterized example is the lysine 40 acetylation (Ac-K40) on α-tubulin (LeDizet and Piperno, 1987; McKeithan and Rosenbaum, 1981). Although this modification always associates with stable MTs, the exact role of Ac-K40 remains elusive. Nonetheless, it has been directly and indirectly implicated in many biological processes, such as primary cilium disassembly, cell migration, and autophagy (Hubbert et al., 2002; Iwata et al., 2005; Pugacheva et al., 2007). Recently, a proteomic study has identified additional acetylations on both α- and β-tubulins (Choudhary et al., 2009). Although the biological significance of these modifications remains to be determined, it suggests that tubulins and MTs may be regulated by multiple acetylation events.

The enzymes that catalyze K40 acetylation and deacetylation have been identified. The Elongator complex is a K40 acetyltransferase while HDAC6 and SirT2 are the deacetylase (Creppe et al., 2009; Hubbert et al., 2002; North et al., 2003; Solinger et al., 2010). Interestingly, these enzymes also modify other proteins and are involved in

other biological processes unrelated to tubulins (Valenzuela-Fernandez et al., 2008). San (Nat5/Nat13/Naa50) is an acetyltransferase required for sister chromatid cohesion in fly and human cells (Hou et al., 2007; Pimenta-Marques et al., 2008; Williams et al., 2003). In addition, San is also a subunit of the N-acetyltransferase NatA complex, which is conserved in eukaryotes (Evjenth et al., 2009). However, San by itself has the acetyltransferase activity and its function in sister chromatid cohesion does not require other subunits of the NatA complex (Hou et al., 2007). San has been shown to acetylate histone H4 in vitro, but whether this acetylation event contributes to sister chromatid cohesion remains unclear (Evjenth et al., 2009).

In an effort to investigate downstream effectors of San, I unexpectedly found that San is a tubulin acetyltransferase, which modifies tubulin heterodimers but not MTs. In HeLa cells, depletion of San does not cause a gross defect in MT cytoskeleton in interphase, but the rate of MT regrowth after catastrophe is significantly increased. San is not responsible for K40 acetylation on α-tubulin. Instead, it catalyzes a novel acetylation on the lysine 252 of β-tubulin. Remarkably, two acetylation-mimicking mutants are incorporated into MTs about 20 fold slower in the same assay. Therefore, I conclude that the K252 acetylation of β-tubulin negatively regulates MT regrowth rate by slowing down the incorporation of the acetylated tubulins.

2.2 Materials and Methods

DNA constructs

Human San constructs in pET28 and pCS2 vectors were described previously (Hou et al., 2007). Human tubulin genes including α (NCBI Reference Sequence: NM_006082), β_I (GenBank: AB062393), and β_{III} (GenBank: BC000748) were amplified from a human thymus cDNA library (Clontech, CA) and subcloned into a modified pCS2 vector. The genes were fused with a carboxyl-terminal flag tag with a TEV cleavage site in between. Site-directed mutagenesis of β_I-tubulin was carried out following the protocol of the QuickChange kit (Stratagene). Human SirT2 gene (NCBI Reference Sequence: NM_012237) was amplified from the same human thymus cDNA library and subcloned into a modified pET28 vector.

Protein preparation

pET28 plasmids carrying San and SirT2 genes were transformed into *E. coli* strain BL21 (DE3). Protein expression was induced by addition of 0.4 mM IPTG at 25°C for 4 hours. 6xHis-tagged proteins were purified using Ni-NTA resins (Qiagen) according to manufacturer's instruction. Briefly, bacteria were spun down and lysed in lysis buffer (50 mM NaH_2PO_4, 300 mM NaCl, 10 mM imidazole, pH 8.0). The lysate was cleared by centrifugation and incubated overnight at 4°C with Ni-NTA resins. The resins were then spun down and packed into a column. The column was washed with lysis buffer followed by wash buffer (50 mM NaH_2PO_4, 300 mM NaCl, 20 mM imidazole, pH 8.0). Proteins were eluted with elution buffer (50 mM NaH_2PO_4, 300 mM NaCl, 250 mM imidazole,

pH 8.0). His_6-San proteins were applied to a S-100 gel filtration column (GE Healthcare) and eluted in modified acetylation buffer (50 mM HEPES, 100 mM NaCl, 10% glycerol, pH 8.0). His_6-SirT2 proteins were dialysed in PBS buffer (140 mM NaCl, 2.7 mM KCl, 10 mM Na_2HPO_4, 1.8 mM KH_2PO_4, pH 7.3).

Bovine tubulin proteins were purchased from Cytoskeleton Inc.. For human tubulin proteins, 293T cells were transfected with tubulin expression plasmids, washed in PBS buffer, and lysed in IP buffer (20 mM Tris pH 7.5, 100 mM NaCl, 0.2% NP-40, 20 mM β-glycine phosphate, 10% glycerol, 1 mM NaF, protease inhibitor cocktail). After centrifugation, the S100 was incubated with anti-flag M2 affinity gel (Sigma-Aldrich) at 4°C for 3 hours. The beads were washed three times in IP buffer followed by modified acetylation buffer (50 mM HEPES, 100 mM NaCl, 10% glycerol, pH 8.0) and the proteins were eluted by one-hour incubation at room temperature in acetylation buffer (50 mM HEPES, 10% glycerol, pH 8.0) containing either 1 mg/ml flag peptide or 2 unit/ml AcTev protease (Invitrogen).

Cell culture and transfection

HeLa and 293T cells were grown in DMEM with 10% fetal bovine serum (FBS) and incubated at 37°C in a 5% CO_2-humidifier chamber. Plasmid DNAs were transfected into HeLa cells using Effectene (Qiagen) according to manufacturer's instruction. 293T cells were transfected using the calcium phosphate precipitation method. Briefly, plasmid DNAs were mixed with 0.25 M $CaCl_2$ solution followed by an equal volume of 2x HBS buffer (50 mM HEPES, 1.5 mM Na_2HPO_4, 140 mM NaCl, 10 mM KCl, 12 mM dextrose,

pH 7.05). The solution was quickly mixed by pipetting and added dropwisely to 293T cells. Medium was changed after 7 hours. Cells were analyzed 48 hours after transfection.

For RNA interference experiments, siRNA oligonucleotides were transfected into HeLa cells at a final concentration of 100 nM using the calcium phosphate precipitation method. Cells were analyzed 72 hours after transfection. The siRNA oligonucleotides A and B (sense/antisense), which were synthesized by GenePharma Co. Inc., are GCUACAAUGACAAGUUCUATT/UAGAACUUGUCAUUGUAGCTG and GCAAUGAGUCGGCAAUUGATT/UCAAUUGCCGACUCAUUGCTG, respectively.

In vitro acetylation assay

The assay was performed in acetylation buffer containing 100 ng/ml His_6-San and 100 mM ^{14}C-labeled acetyl-CoA (PerkinElmer). After one hour incubation at 37°C, 5x SDS-PAGE loading buffer (250 mM Tris-HCl pH 6.8, 50% glycerol, 10% SDS, 10% β-mercaptoethanol, 1% bromophenol blue) was added to terminate the reaction. After resolving the proteins by SDS-PAGE, acetylation was detected by exposing the gel to phosphor image screen.

Affinity purification of San substrates and identification of tubulin

His_6-San proteins were covalently conjugated to NHS (N-hydroxysuccinimide)-activated Sepharose beads (GE Healthcare). 200 μl of NHS beads were washed with 1 ml of cold HCl followed by 5 ml of cold distilled water. The beads were incubated overnight at 4°C with 3 mg of His_6-San. Tris buffer (1 M Tris-HCl pH 8.0) was added to the slurry at a final concentration of 0.1 M and incubated at room temperature for 1 hour to

deactivate reactive sites of NHS beads. The beads were then washed three times with 5 bed-volume of PBS buffer followed by column storage buffer (50 mM Tris-HCl pH 7.5, 0.02% NaN_3). The beads were stored in column storage buffer at 4°C and equilibrated with acetylation buffer before use. HeLa cells were lysed in acetylation buffer using a nitrogen bomb. After centrifugation at 50,000g, 600 μl of supernatant was incubated overnight at 4°C with 0.5 ml of either San-conjugated beads or empty beads. Beads were washed three times with acetylation buffer, and proteins bound to the beads were subjected to in vitro acetylation assay. For the empty beads control, His_6-San was added after the pull down experiment. After resolving the proteins by SDS-PAGE, the gel was stained by Coomassie Blue and exposed to phosphor image screen. A ~50 kD protein band extensively labeled by ^{14}C was sliced out and sent for mass spectrometry. It was identified as α/β tubulin heterodimer by UT Southwestern Protein Chemistry Technology Center using HPLC/MS/MS.

SDS-PAGE and immunoblotting

Protein samples and whole cell lysates were dissolved in 1x SDS-PAGE loading buffer and heated at 95°C for 5 minutes. The samples were resolved through 5-15% SDS-PAGE gradient gels. For Coomassie Blue staining, gels were washed in distilled water and stained by GelCode Blue (Pierce). For immunoblotting, proteins were transferred to nitrocellulose membranes, blocked with 5% dry milk, and incubated with indicated primary antibodies. Antibodies used for immunoblotting were as following: anti-flag (Sigma-Aldrich) 1:2000, anti-Ac-K40 of α-tubulin (Sigma-Aldrich) 1:10000, anti-α-tubulin (Sigma-Aldrich) 1:2000, anti-β-tubulin (Sigma-Aldrich) 1:500, anti-actin (Sigma-

Aldrich) 1:2000, anti-Erk2 (Santa Cruz) 1:1000, and anti-San (Hou et al., 2007) 1:1000. Signals were detected by incubation with HRP-conjugated secondary antibodies (Jackson ImmunoResearch) followed by SuperSignal West Pico Chemiluminescent Substrate (Pierce).

MT regrowth assay, immunofluorescence staining and microscopy

Cells seeded on cover slips were put on ice for 30 minutes to depolymerize MTs. Cover slips were then incubated in pre-warmed medium at 37°C for indicated time, followed by fixation in cold methanol at -20°C. For immunofluorescence staining, cover slips were washed three times in PBS buffer, blocked with 3% bovine serum albumin (BSA) dissolved in PBS, and incubated with indicated primary antibodies. Antibodies used for immunofluorescence staining were as following: anti-flag 1:1000, anti-α-tubulin 1:1000, anti-San 1:100, and anti-γ-tubulin (Sigma-Aldrich) 1:500. After three washes in PBS buffer, the cover slips were incubated with Cy3 and Alexa Fluor 488–labeled secondary antibodies (Invitrogen) and DAPI (4',6-diamidino-2-phenylindole) (Invitrogen), followed by another three washes in PBS buffer. The cover slips were mounted with Aqua Polymount (Polysciences). Epifluorescence microscopy was performed on an Axio Observer Z1 microscope. A Plan-Apochromat 63x/1.40 Oil DIC M27 objective was used, and images were acquired with an AxioCam MRm rev. 1-3 camera controlled by AxioVision software. Gamma adjustment and necessary cropping were performed using Adobe Photoshop CS2.

Statistical analysis

Statistical analyses were performed using Microsoft Excel. One-tail unpaired Student's t-test was performed, and data sets were considered significantly different with $p<0.05$.

2.3 Results

San acetylates tubulin

To identify San substrates, NHS-sepharose beads conjugated with recombinant San proteins were incubated with cytoplasmic fractions prepared from HeLa cells. After three washes, the beads were incubated with ^{14}C-acetyl-CoA to radiolabel potential substrates. On SDS-PAGE, a ~52 kD band exhibited the most prominent signal on the Coomassie Blue stained gel and the phosphor image (Fig. 2.1A). The band was sliced out and mass spectrometry analysis identified it as α- and β-tubulin. To directly validate tubulin as a San substrate, I performed the in vitro acetylation assay using commercial bovine tubulin. As shown in Fig. 2.1B, tubulin was acetylated by San, but not acetyltransferase ESCO2 (Hou and Zou, 2005), indicating that San specifically acetylates tubulin. Interestingly, San did not acetylate taxol-stabilized MT (Fig. 2.1C), suggesting that the targeted residue is inaccessible on MTs or San does not interact with MTs. Taken together, San is a tubulin acetyltransferase (TAT) that specifically modifies tubulin heterodimers.

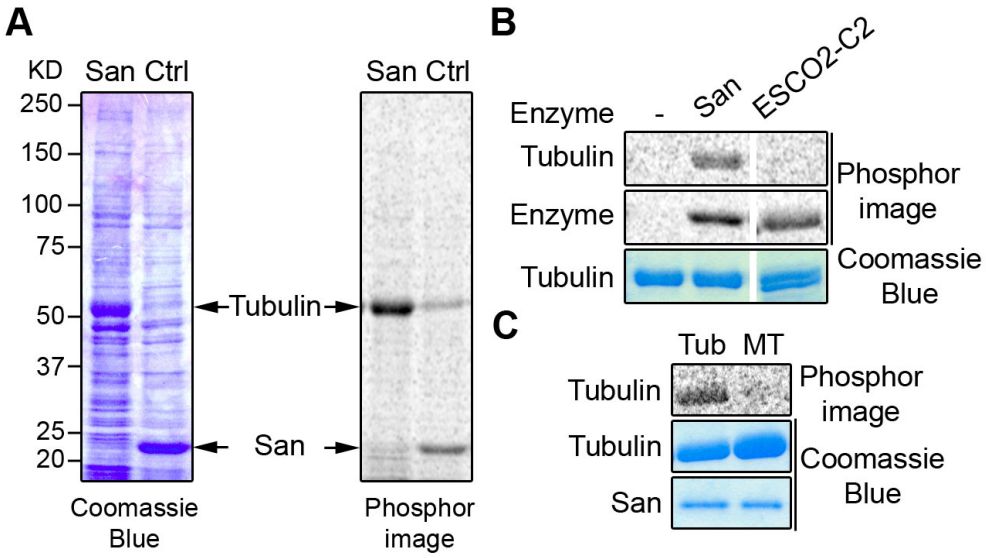

Figure 2.1. San acetylates tubulin heterodimers but not microtubules in vitro.

A. Tubulin is a San substrate. HeLa cell lysate was incubated with either San-conjugated NHS beads (San) or empty beads (Ctrl). Proteins bound to the beads were subjected to in vitro acetylation with San. For the empty beads control, recombinant San was added after the pull down experiment. After resolving the proteins by SDS-PAGE, the gel was stained by Coomassie Blue (left panel) and exposed to phosphor image (right panel). The 52 KD protein band was identified as tubulin by mass spectrometry. **B**. Tubulins were acetylated by San but not ESCO2. Bovine tubulins were subjected to in vitro acetylation with buffer (-), San or ESCO2. The tubulin doublet shown in the third lane was due to partial separation of α- and β-tubulin on the gel. The self-acetylations of San and ESCO2 were used as controls for enzymatic activity. **C**. Tubulins but not microtubules were acetylated by San. Microtubules made of bovine tubulins were either depolymerized to tubulins by incubation on ice (Tub) or stabilized by taxol (MT). Both preparations were subjected to in vitro acetylation with San.

San slows down tubulin regrowth after cold-induced catastrophe

To investigate how the San-catalyzed tubulin acetylation affects MT functions in vivo, I first overexpressed San in HeLa cells (Fig. 2.2A), and no obvious MT abnormality was detected (Fig. 2.2B). It is possible that the activity of San is tightly regulated. I also knocked down San expression to about 20% of the physiological level in HeLa cells using two siRNA oligonucleotides (Fig. 2.3A). Again, no obvious defects in MT cytoskeleton were detected in interphase cells (Fig. 2.3B). In mitosis the spindle was disorganized as previously reported (Hou et al., 2007), but it could be caused by premature sister chromatid separation (Dai et al., 2009). Next, I investigated whether MT dynamics is affected by depleting San. To this end, I performed the cold-induced MT depolymerization and regrowth assay to analyze the rate of MT depolymerization and polymerization. After examining the MT staining at different time points, no significant difference in the rate of MT depolymerization was detected when cells were incubated at 4°C (Fig. 2.3C). However, after cells were put back to 37°C incubation, the rate of MT regrowth from the centrosome was noticeably faster in San-siRNA cells. The difference was quantified as the percentage of cells with centrosomal MT asters 1.5 minutes after temperature shift (Fig. 2.3D). Centrosomal MT asters appeared in about 25% of the mock-treated cells, but in about 40% of the San-siRNA cells (Fig. 2.3E). At 2.5 minutes, near 100% of cells with or without siRNA transfection contained centrosomal MT asters (data not shown). Taken together, these results indicate that San negatively affects the rate of MT polymerization/nucleation.

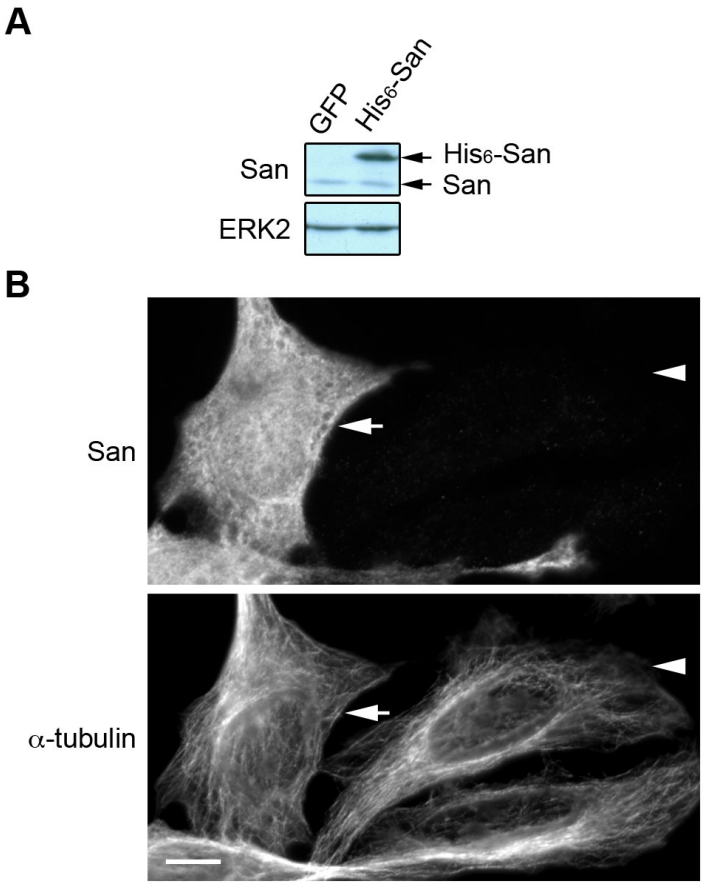

Figure 2.2. Overexpression of San did not affect microtubule organization in vivo.

A. Overexpression of His_6-San in HeLa cells. Protein extracts of cells transfected with GFP or His_6-San plasmids were analyzed by immunoblot and probed for San. ERK2 was probed as the loading control. **B.** Representative images of cell with (arrow) or without (arrowhead) His_6-San overexpression. HeLa cells transfected with His_6-San plasmids were stained to visualize San and microtubules (α-tubulin). Scale bar, 10 μm.

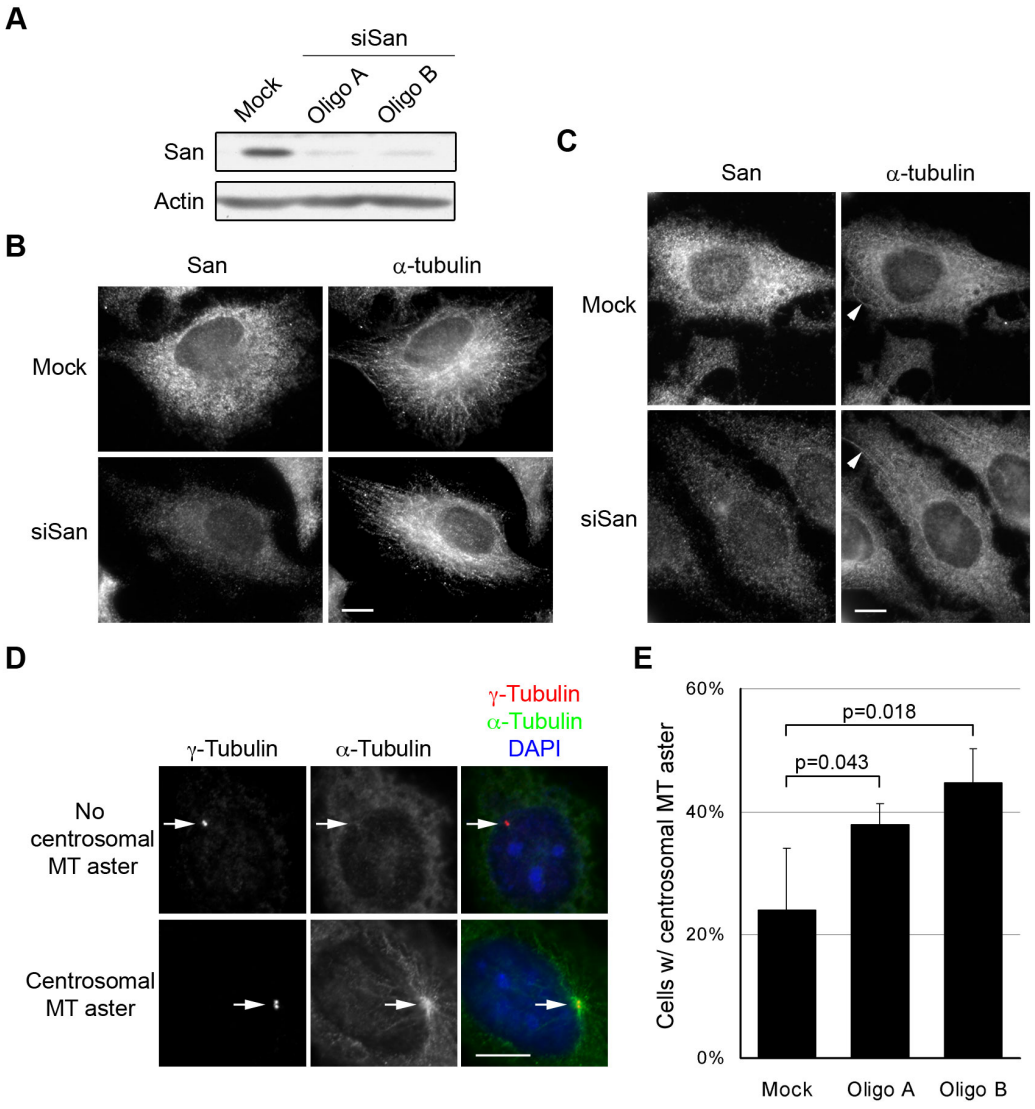

Figure 2.3. Centrosomal microtubule regrowth is accelerated in San-depleted cells.

A. San protein level was decreased by RNAi. Protein extracts of HeLa cells transfected with mock or two siRNA oligoes (A and B) targeting San were analyzed by immunoblot and probed for San. Actin was probed as the loading control. **B.** San depletion did not affect microtubule organization in vivo. HeLa cells transfected as in **A** were stained to visualize San and microtubules (α-tubulin). Scale bar, 10 μm. **C.** San depletion did not affect the rate of cold-induced microtubule depolymerization in vivo. HeLa cells transfected as in **A** were incubated on ice for 15 minutes, followed by fixation and immunofluorescence staining to visualize San and microtubules

(α-tubulin). Arrowheads mark residual MT staining. Scale bar, 10 μm. **D.** Representative images of cell with or without centrosomal microtubule aster in the microtubule regrowth assay. HeLa cells synchronized to G1/S phase were incubated on ice to depolymerize microtubules, followed by incubation in warm medium for 1.5 minutes to allow regrowth of microtubules from the centrosome. Cells were stained to visualize centrosomes (γ-tubulin, red), microtubules (α-tubulin, green), and DNA (DAPI, blue). Arrows mark centrosomes. Scale bar, 10 μm. **E.** Quantification of cells with centrosomal microtubule asters. For each sample, at least 50 cells were counted and the average percentage of cells with centrosomal microtubule aster was determined from three independent experiments. Error bars indicate SD.

San does not acetylate α-tubulin at lysine 40

To investigate whether the faster MT reassembly in San-siRNA cells is related to the reduced level of San-catalyzed tubulin acetylation, I mapped the acetylation site so that mutations could be introduced to block and/or mimic the acetylation. First, I examined whether the acetylation is at the well-characterized lysine 40 on α-tubulin. To this end, I compared the Ac-K40 level in normal and San-siRNA cells. Using an Ac-K40 specific monoclonal antibody, I did not detect any change upon San depletion (Fig. 2.4A). Therefore, it is unlikely that San is the major acetyltransferase that acetylates K40. To directly test whether K40 acetylation can be catalyzed by San, I removed K40 acetylation from bovine tubulin using recombinant SirT2, one of the two deacetylases targeting Ac-K40 (North et al., 2003). After incubation with SirT2, the bovine tubulin became free of Ac-K40 (Fig. 2.4B, lane 2). Next, the deacetylated tubulin was re-acetylated by San in the presence of ^{14}C-acetyl-CoA and nicotinamide (NAM), a SirT2 inhibitor. I detected marked increases in total tubulin acetylation, measured by ^{14}C incorporation. However the level of Ac-K40, measured by immunoblot using the Ac-K40 antibody, remained undetectable (Fig. 2.4B, lane 6). This indicates that San catalyzes a

different acetylation from K40 acetylation. Furthermore, the level of ^{14}C incorporation was indistinguishable from that in the absence of NAM (Fig. 2.4B, lane 4), suggesting that, unlike K40 acetylation, the acetylation catalyzed by San is resistant to SirT2. Taken together, I conclude that San does not catalyze the acetylation of K40 on α-tubulin.

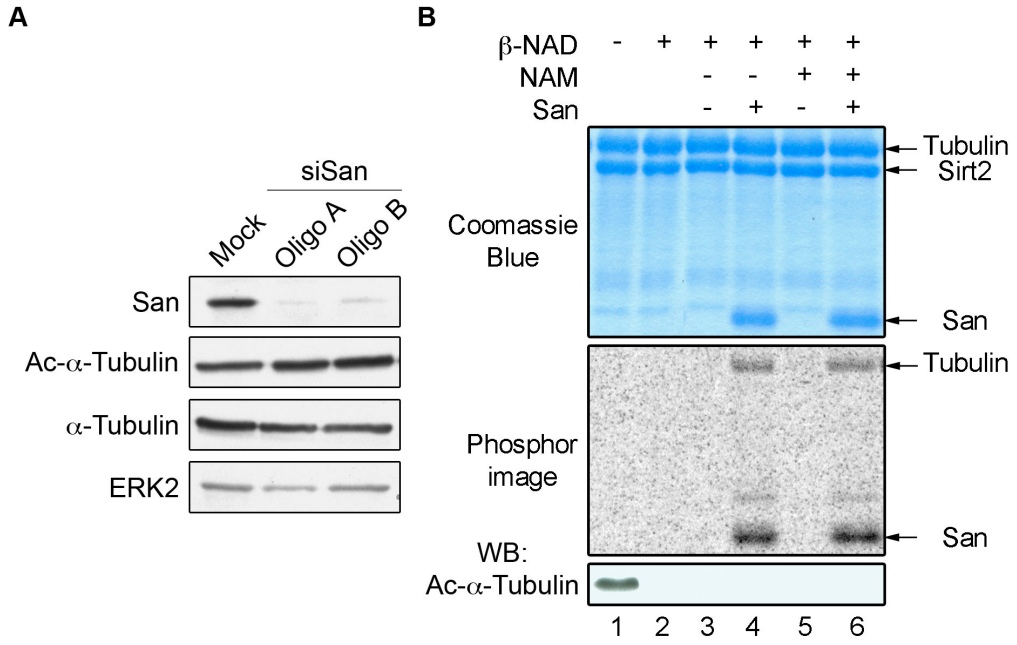

Figure 2.4. San does not acetylate α-tubulin K40.

A. K40 acetylation level was unchanged in San-siRNA cells. Protein extracts of San-siRNA HeLa cells were analyzed by immunoblot. ERK2 was probed as the loading control. **B.** San-medicated acetylation on tubulin was not at α-tubulin K40. Bovine tubulins were incubated with His_6-SirT2 and β-NAD to deacetylate α-tubulin K40 (lane 2). These deacetylated tubulins were then subjected to the in vitro acetylation in the presence or absence of San and NAM (lane 3-6). Proteins were analyzed by Coomassie Blue staining, phosphor-imaging and immunoblot.

San acetylates β-tubulin at lysine 252

Having demonstrated that San-catalyzed tubulin acetylation was previously uncharacterized, I investigated which tubulin subunit was acetylated. I cloned the ubiquitous isotype of α-tubulin and the ubiquitous β-tubulin isotype I (β_I) and added a flag tag at their carboxyl-termini. The tagged tubulins were expressed in 293T cells, immunopurified on anti-flag beads, and eluted with flag peptides. Next, the purified tubulins were incubated with recombinant San in the presence of ^{14}C-acetyl-CoA. As shown in Fig. 2.5A, San acetylated only β-tubulin. The acetylation was also detected on the neuronal-specific isotype β_{III}, suggesting that the acetylation might not be isotype-specific. Taken together, I conclude that San is a β-tubulin TAT.

To map the acetylation site on β-tubulin, I prepared recombinant β_I-tubulin-flag from 293T cells. After incubation with San for two hours, β_I-tubulin-flag was separated from San by SDS-PAGE, sliced out of the gel, and analyzed by mass spectrometry. Acetylation at lysine 252 (K252) was detected on several peptides (Chu et al., submitted). In addition, acetylation at lysine 324 (K324) was also suggested but with a much lower confidence (data not shown). Acetylations at these two sites were later identified in vivo on β_I-tubulin purified from hTert-RPE1 cells (Chu et al., submitted). To investigate whether these acetylations were catalyzed by San, I constructed K-to-A or K-to-R mutations at these two sites and compared the acetylation of the mutants with that of the wild type. As shown in Fig. 2.5B, the K324R mutation did not significantly reduce the level of acetylation, indicating that K324 is not the primary site modified by San. On the other hand, acetylation of the K252A mutants was reduced to approximately 30% of that

of the wild type. The residual labeling was presumably attributed to the N-acetyltransferase activity of San (Evjenth et al., 2009), because the signal was comparable with that of the 15KRA mutant, in which all 15 lysines are substituted with arginines or alanines. In addition, I also analyzed the in vitro acetylation at lysine 58 (K58), which was recently identified as being acetylated in vivo (Choudhary et al., 2009). The K58R mutation did not reduce the level of acetylation in vitro (Fig. 2.5C), indicating that this is not a San target site. Taken together, these results indicate that β-tubulin is acetylated at multiple sites in vivo and, among them, the K252 acetylation is specifically catalyzed by San.

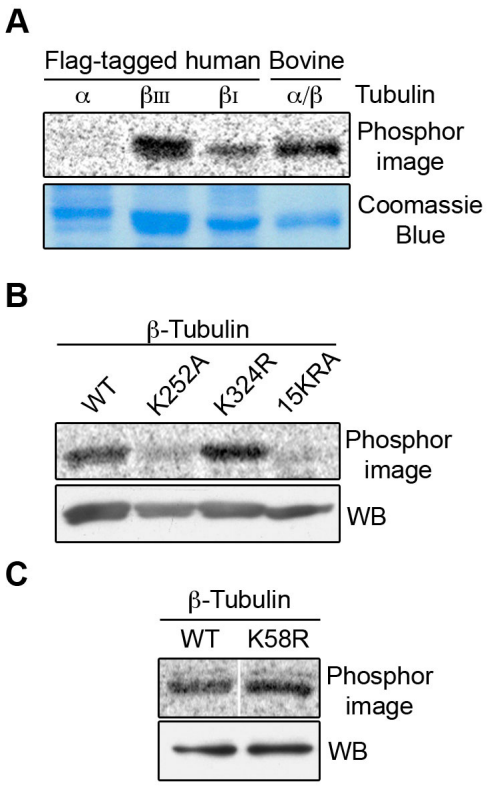

Figure 2.5. San acetylates β-tubulin K252.

A. San acetylated β- but not α-tubulin. Flag-tagged tubulins were expressed in 293T cells, purified on anti-flag affinity gel, and analyzed by the in vitro acetylation assay. Bovine tubulin serves as a positive control. **B. and C.** β-tubulin K252A mutant was not efficiently acetylated by San in vitro. Wild type and mutant β-tubulins were expressed in 293T cells, purified on anti-flag affinity gel, eluted by TEV protease, and analyzed by the in vitro acetylation assay. Immunoblot with β-tubulin antibody demonstrated equal loading. β-tubulin K58 was shown acetylated in vivo, but the K58A mutant did not reduce San-mediated acetylation in vitro.

The acetylation-mimicking tubulin mutants form heterodimers in vivo and are incorporated into MTs

Because MT regrowth is accelerated in San-siRNA cells, I decided to investigate the incorporation rate of the K252A/Q and K252R mutants, which were designed to mimic the acetylated and unacetylated β-tubulin respectively. First, I examined whether the tubulin mutants were able to form heterodimers with α-tubulin. To this end, I expressed flag-tagged mutants in 293T cells and found that neither K252A/Q nor K252R mutant co-immunoprecipitated with α-tubulin (Fig. 2.6A), indicating the mutations may destabilize the tubulin heterodimers. Nonetheless, these mutants were incorporated into MTs when expressed in HeLa cells. As shown in Fig. 2.6B, expression of the mutants in HeLa cells did not cause any detectable change in total β-tubulin levels, indicating that they were expressed at very low level compared to the endogenous β-tubulin. Similar to the wild-type control, the K252A/Q mutants were incorporated into MTs (Fig. 2.6C), indicating that the mutations did not cause gross changes in tubulin conformation and formed functional heterodimers in vivo. Furthermore, cells expressing the mutant tubulins were indistinguishable from that expressing the wild-type tubulins. Taken together, the lack of obvious phenotype indicated that these mutants were unlikely to sequester tubulin chaperones. The K252R mutant behaved differently. In about 50% of the transfected cells, this mutant was also detected on seemingly normal MTs. In the rest of the cells, the MT cytoskeleton became disorganized and/or disintegrated (Fig. 2.7A). The phenotype was also observed in mitotic cells where above 50% of the mitotic spindles become multipolar and away from the center of the cell (Fig. 2.7B). Although

cells with abnormal MTs usually exhibited higher expression level of the K252R mutant, this was not always the case. Nor did the phenotype correlate with the duration of expression. Currently, the reason that cells respond differently to the expression of the K252R mutant remains unsolved.

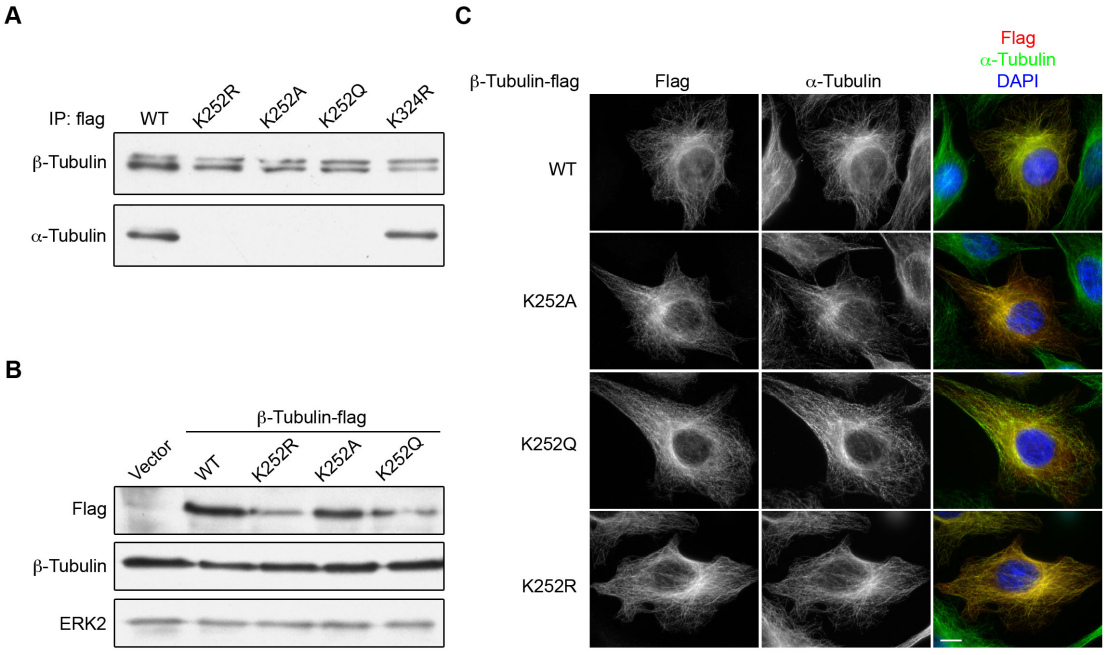

Figure 2.6. β-tubulin K252 mutants are incorporated into microtubules in HeLa cells

A. The β-tubulin K252 mutants exhibit weaker binding to α-tubulin in vitro. Flag-tagged wild type and mutant β-tubulins were expressed in 293T cells, purified on anti-flag affinity gel, eluted by TEV protease, and analyzed by immunoblot. The doublet of β-tubulin blot was a result of partial cleavage by TEV protease. **B.** Protein level of β-tubulin mutants. Protein extracts of HeLa cells transfected with indicated plasmids were analyzed by immunoblot. ERK2 was probed as the loading control. **C.** Cellular localization of tubulin mutants in HeLa cells. Cells transfected with indicated plasmids were stained to visualize tubulin mutants (flag, red), microtubules (α-tubulin, green) and DNA (DAPI, blue). Representative images are shown. Scale bar, 10 μm.

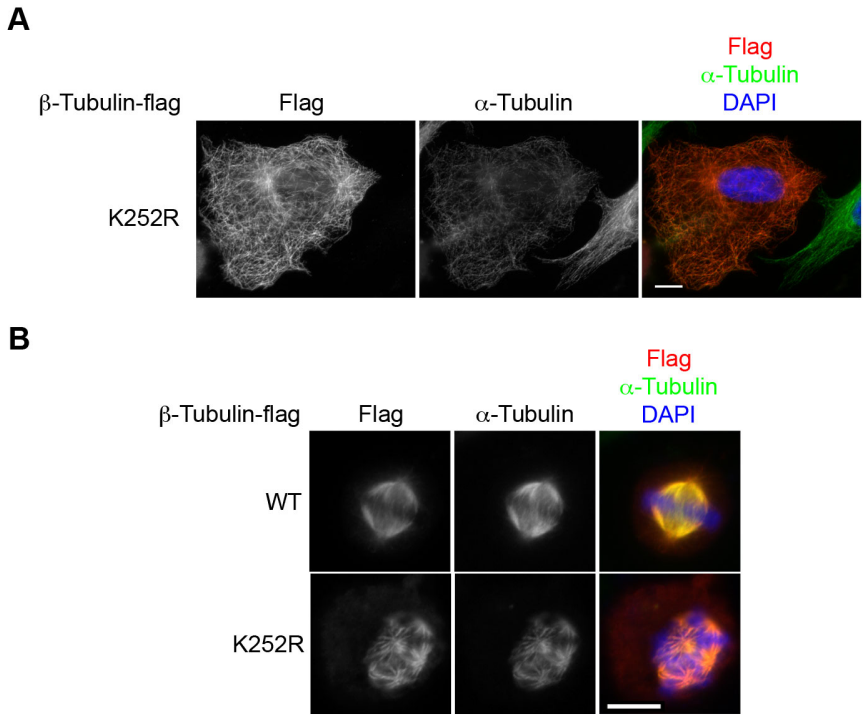

Figure 2.7. β-tubulin K252R mutant disrupts microtubule cytoskeleton in interphase and mitotic cells.

HeLa cells expressing the K252R mutant were stained to visualize tubulin mutants (flag, red), microtubules (α-tubulin, green) and DNA (DAPI, blue). Representative images are shown. Expression of the K252R mutant had two distinct effects on interphase microtubule organization (**A**) and affected mitotic spindle organization (**B**). Scale bar, 10 μm.

The acetylation-mimicking mutants are incorporated into regrowing MTs with a much slower rate

Because the acetylation-mimicking mutants were capable to be incorporated into MTs, I next performed MT regrowth assay to analyze their incorporation rates. In HeLa cells expressing these flag-tagged tubulins, no defects were detected regarding the

formation of centrosomal asters, which was detected in near 100% of the cells after shifting the culture back to 37°C for 2.5 minutes (data not shown). This was expected because the low expression levels of the mutants were unlikely to dominant-negatively affect the overall MT dynamics. The K252R mutant did not incorporate faster than the wild type, as one might predict based on the phenotype of San-siRNA cells. Instead, its incorporation rate is between that of the wild type and the K252A/Q mutants. It is possible that this mutant does not fully mimic the unacetylated form. On the other hand, the acetylation-mimicking K252A/Q mutants were detected at the centrosomes in less than 2% of the expressing cells (Fig. 2.8A and B). At this time point, the wild type β-tubulin-flag was detected at the centrosomes in near 100% of the cells. After 30 minutes, K252A and K252Q were incorporate into centrosomal and/or cytoplasmic MTs in 54% and 11% of the cells, respectively. At the 60-minute time point, the mutants were incorporated in all the cells and became indistinguishable from the flag-tagged wild type tubulin (Fig. 2.9). This represented a greater than 20-fold difference in the rate of incorporation. The slower incorporation rate of the acetylation-mimicking mutants suggests that K252 acetylation on β-tubulin may severely delay their incorporation into the growing MT. This observation is consistent with the accelerated MT regrowth in San-siRNA cells (Fig. 2.3E).

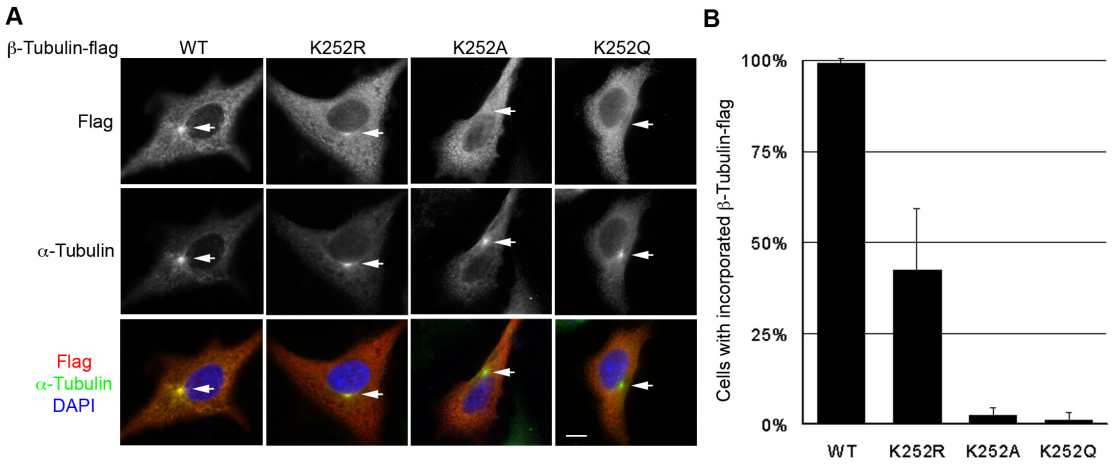

Figure 2.8. Incorporation of the acetylation-mimicking β-tubulin mutants is delayed in the MT regrowth assay.

A. β-tubulin K252A and K252Q mutants were not incorporated into centrosomal microtubule asters. HeLa cells expressing indicated tubulin mutants were subjected to the microtubule regrowth assay, fixed after 2.5 minutes of regrowth, and stained to visualize tubulin mutants (flag, red), microtubules (α-tubulin, green), and DNA (DAPI, blue). Representative images are shown. Arrows mark centrosomal microtubule asters. Scale bar, 10 μm. **B.** Quantification of cells with flag-positive centrosomal microtubule asters. In each sample, at least 50 cells were counted, and the average percentage of flag-expressing cells with flag-positive centrosomal microtubule asters was determined from three independent experiments. Error bars indicate SD. Between wild type and all three mutants, $p<0.001$.

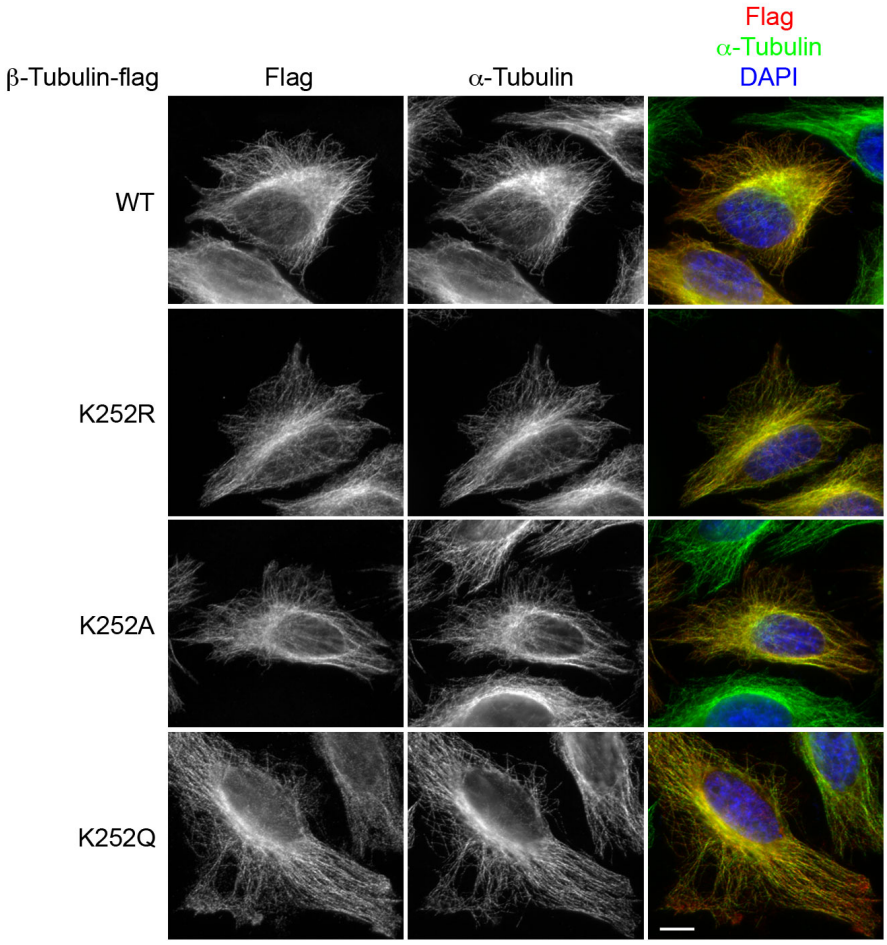

Figure 2.9. β-tubulin K252 mutants are incorporated into microtubules after cold treatment in HeLa cells.

HeLa cells expressing indicated tubulin mutants were subjected to the microtubule regrowth assay. After 60 minutes of regrowth, cells were stained to visualize tubulin mutants (flag, red), microtubules (α-tubulin, green) and DNA (DAPI, blue). Representative images are shown. Scale bar, 10 μm.

2.4 Discussion

Previous studies have implicated San in N-terminal acetylation and sister chromatid cohesion in metazoans. Here I demonstrated that San acetylates β-tubulin and negatively regulates tubulin incorporation. Unlike most tubulin modifications, the acetylation is only added to free tubulin heterodimers but not to taxol-stabilized MTs. This is similar to a previously described β-tubulin phosphorylation that also inhibits tubulin incorporation (Fourest-Lieuvin *et al.*, 2006). My findings thus provide another example of tubulin posttranslational modification directly regulating MT dynamics.

Manipulation of San protein level in HeLa cells did not affect MT organization or MT stability. Compared to San-depleted cells that exhibited accelerated centrosomal MT regrowth, San-overexpressing cells showed no difference in terms of centrosomal MT regrowth (data not shown). Three possibilities may contribute to the lack of phenotype. One is that not all the overexpressed San proteins were available for tubulin. Endogenous San proteins are restricted within the cytoplasm, while overexpressed San proteins are evenly distributed in the whole cell including nucleus (Fig. 2.2B, 2.3B). This distribution pattern is not due to the flag tag, because non-tagged San displays the same pattern when overexpressed (data not shown). Since most tubulins locate in the cytoplasm, those San proteins locating in the nucleus will have no access to tubulin unless they are exported and remain catalytically active. The other possibility is the presence of a San inhibitor, which will be described in the next chapter. Taken together, it is possible that the protein level of overexpressed San was not enough to overcome the inhibitory effect on San. The last possibility is that the amount of San is not the limiting

factor of San-catalyzed tubulin acetylation, i.e. the endogenous level of San is already higher than necessary. In this case, overexpressing San will not increase San-catalyzed tubulin acetylation, and only an efficient depletion of San will significantly decrease the tubulin acetylation.

The San-catalyzed acetylation in vitro was mapped on the lysine 252 of β-tubulin. San is likely to catalyze this acetylation in vivo, as supported by the following evidence. Firstly, K252 is found acetylated in vivo (Chu et al., submitted). Secondly, depletion of San increases the rate of MT regrowth in vivo, suggesting that San regulates tubulin functions. Finally, the K252A/Q mutants, which mimic the acetylated tubulins, are incorporated into MTs with a much slower rate, suggesting that the K252 acetylation impedes tubulin polymerization. A K252 acetylation specific antibody will provide the direct evidence that the K252 acetylation is catalyzed by San in vivo.

β-tubulin K252 locates at the interface between tubulin heterodimer (Fig. 2.10). The residue is in a region that has been shown involved in taxol-induced MT stabilization, and it is also in proximity to the binding pocket of MT depolymerizing drug colchicine (Ravelli et al., 2004; Xiao et al., 2006). The acetylation on K252, which removes the charge of the lysine residue, may cause a conformational change of the heterodimer and result in the delay in tubulin incorporation. Interestingly, the positive charge at the side chain of K252 was proposed to neutralize the negative charge of the α-tubulin-bound GTP and stabilize the heterodimer (Lowe et al., 2001). Consistent with this proposal, the acetylation-mimicking mutants forms a less stable heterodimer as demonstrated in the co-immunoprecipitation assay (Fig. 2.6A).

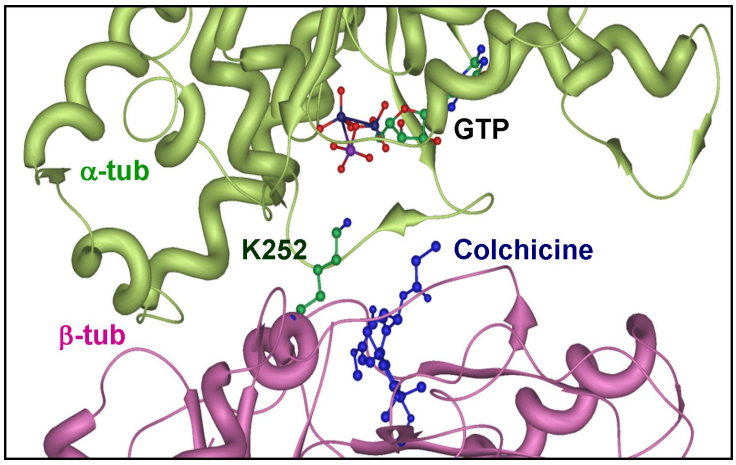

Figure 2.10. The position of β-tubulin K252 on the structure of tubulin heterodimer.

The structure is obtained from the tubulin in complex with colchicine and the stathmin-like domain of RB3 (PDB: 1SA0). The α-tubulin-bound GTP, β-tubulin K252 and colchicine are displayed as ball-and-stick structure.

β-tubulin k252R mutant, presumably mimicking the unacetylated tubulin, did not behave as the opposite of the K252A/Q mutants. Although the K252R mutant was incorporated faster than the K252A/Q mutants in the MT regrowth assay, it did not match or exceed the incorporation rate of wild type. In half of the mutant-expressing cells, incorporation of the K252R mutant caused MT disorganization and destabilization, characterized by decreased immunostaining signal of α-tubulin and α-tubulin K40 acetylation (Fig. 2.7, data not shown). This phenotype may be due to the decreased heterodimer stability of the K252R mutant. I suspect that the K252R mutant does not fully resemble the unacetylated tubulin. Because K252 locates at the heterodimer interface, the side chain of arginine, which is larger than that of unacetylated lysine, may

generate steric hinderance within the interface. As a result, the substitution may have an impact on heterodimer formation and result in an abnormal conformation even after the heterodimers are integrated into MTs. Incorporation of such mutant tubulins may create some structurally weak points and eventually lead to MT catastrophe.

Tubulin heterodimers exist in at least two conformations. It adopts the straight conformation when they are polymerized into MTs (Nogales et al., 1998). On the other hand, depolymerized tubulins adopt a curved conformation (Gigant *et al.*, 2000; Wang and Nogales, 2005; Rice *et al.*, 2008). Curved tubulins are straightened during incorporation into MTs and mechanisms impeding this conformational change negatively regulate MT polymerization. For example, MT destabilizing factor stathmin decreases MT polymerization by binding to and stabilize tubulin heterodimers in the curved conformation (Jourdain *et al.*, 1997; Gigant *et al.*, 2000). Based on my findings, I propose that the San-catalyzed β-tubulin K252 acetylation impedes tubulin incorporation by abolishing the K252-GTP interaction and inducing the modified tubulins to adopt a conformation that disfavors MT polymerization (Fig. 2.11). Therefore, the acetylation-mimicking K252A/Q mutants may start to be incorporated into MTs only after most of the wild type tubulins have been integrated. This explains the delay observed in the MT regrowth assay. Such a model also explains the increased rate of MT regrowth in San-siRNA cells, where more tubulins are unacetylated and easily adopt the straight conformation during polymerization.

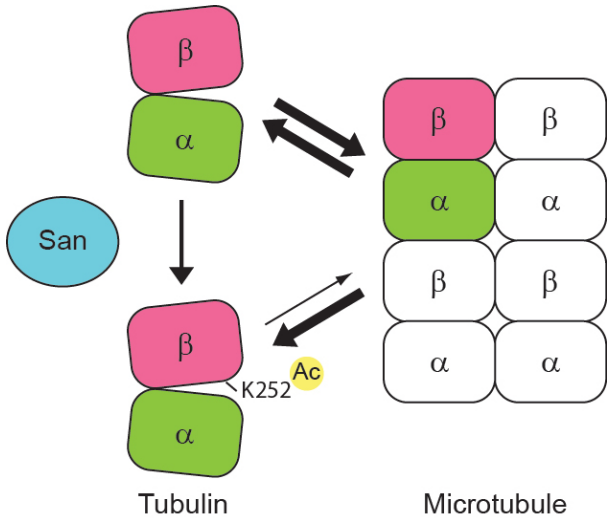

Figure 2.11. A schematic model illustrating the effect of San on microtubule assembly.

San-catalyzed acetylation at β-tubulin K252 impedes tubulin polymerization by abolishing the K252-GTP interaction and inducing conformational changes which prevent modified tubulins from adopting the straight conformation.

CHAPTER THREE

CHARACTERIZATION AND PURIFICATION OF THE ENDOGENOUS SAN INHIBITOR

3.1 Introduction

Acetylation is commonly detected on many proteins and involved in various cellular events. Lysine acetylation, catalyzed by lysine acetyltransferases (KATs), is implicated in gene transcription, signal transduction and cell migration (Yang and Seto, 2008). Tight regulation of the activity of KATs is critical for cells to function properly, and many acetylation events are deregulated in cancer cells (Yang and Seto, 2007). KATs usually work as protein complexes, and their activity and substrate specificity are modulated by the regulatory subunits as well as various posttranslational modifications (Mellert and McMahon, 2009).

San (Nat5/Nat13/Naa50) is an acetyltransferase required for centromeric cohesion and chromosome resolution in *Drosophila* and human (Hou et al., 2007; Pimenta-Marques et al., 2008; Williams et al., 2003). San by itself can catalyze both N-terminal acetylation and lysine acetylation (Evjenth et al., 2009). In spite of being a subunit of the N-acetyltransferase NatA complex, the function of San in sister chromatid cohesion is independent of the function of NatA (Hou et al., 2007). San acetylates itself in an intramolecular manner, and the autoacetylation affects its substrate specificity (Evjenth et al., 2009; Hou et al., 2007). In addition to autoacetylation, San also acetylates histone H4 and β-tubulin (Evjenth et al., 2009) (Chu et al., submitted). Nevertheless, how

the activity of San is regulated in vivo remains elusive, given that the protein level of San appears unregulated temporally or spatially during the cell cycle progression (Evjenth et al., 2009; Hou et al., 2007).

Here I present evidence indicating the existence of a protein-based San inhibitor in cell lysates. ATP is a necessary cofactor for the inhibition to happen, but ATP hydrolysis is not required. I partially purified this inhibitor by ammonium sulfate fractionation and ATP-conjugated resin. Besides, gel filtration chromatography suggests that this inhibitor may be a multi-subunit protein complex.

3.2 Materials and Methods

Autoacetylation assay of San

Unless further noticed, the assay was performed in acetylation buffer containing the protein lysates, 50 ng/μl His_6-San and 100 μM ^{14}C-labeled acetyl-CoA (PerkinElmer). After one hour incubation at 37°C, 5x SDS-PAGE loading buffer (250 mM Tris-HCl pH 6.8, 50% glycerol, 10% SDS, 10% β-mercaptoethanol, 1% bromophenol blue) was added to terminate the reaction. After resolving the proteins by SDS-PAGE, acetylation was detected by exposing the gel to phosphor image screen.

Subcellular fractionation

HeLa cells were lysed in acetylation lysis buffer (50 mM HEPES pH 8.0, 100 mM NaCl, 10% glycerol, 1 mM DTT, protease inhibitor cocktail) using a nitrogen bomb. After centrifugation at 100,000g, the supernatant (S100) was collected and the pellet

(P100) was suspended in equal volume of acetylation buffer. To separate small molecules from proteins in S100, 2.5 ml of S100 was applied to a PD-10 desalting column (GE Healthcare). Proteins (P) were eluted with 3.5 ml of acetylation buffer, followed by elution of small molecules (SM) with another 3.5 ml of acetylation buffer. The fractions were subjected to the autoacetylation assay of San, and the following compounds were added to their final concentrations as indicated: 1 mM ATP, 1 mM GTP, 1 mM ATPγS, 5 mM $MgCl_2$, and 10 mM EDTA. Proteins were resolved by SDS-PAGE and exposed to phosphor image screen.

Ammonium sulfate fractionation

Saturated (100%) ammonium sulfate solution in 20 mM Tris pH 8 was added to HeLa cell S100 at a final concentration of 20% and incubated on ice for 1 hour. After centrifugation at 5,000g, the pellet was collected (0-20%) and 100% ammonium sulfate solution was added to the supernatant at a final concentration of 40%. After incubation on ice and centrifugation as mentioned above, the pellet was collected (20-40%) and the supernatant was mixed with 10-fold volume of 100% ammonium sulfate solution. After incubation on ice and centrifugation, the pellet was collected (40-100%) and the supernatant was discarded. To remove ammonium sulfate from proteins, all the pellets were dissolved in equal volume of modified acetylation buffer, applied to PD-10 columns, and eluted with modified acetylation buffer. All the fractions were subjected to the autoacetylation assay of San in the presence or absence of 1 mM ATP, resolved by SDS-PAGE, and exposed to phosphor image screen.

Affinity purification of the San inhibitor using ATP resin

120 μl of HeLa cell 40-100% ammonium sulfate fraction was mixed with equal volume of 2x ATP binding buffer (2x modified acetylation buffer, 0.1% NP-40, 2mM DTT, 2x protease inhibitor cocktail, 2 mM ADP, 2 mM AMP, 2 mM NADH) and incubated with 30 μg of pre-equilibrated ATP-Binders resin (Novagen) at 4°C for 3 hours. After three washes with ATP binding buffer, proteins bound to the resin were eluted three times with 40 μl of ATP elution buffer (modified acetylation buffer, 20 mM ATP) each time. All the eluants were subjected to the autoacetylation assay of San, resolved by SDS-PAGE, and exposed to phosphor image screen.

Purification of the San inhibitor using gel filtration chromatography

After centrifugation and filtering through a 0.22 μm filter, 5 ml of HeLa cell 40-100% ammonium sulfate fraction was applied to an equilibrated Superdex 200 gel filtration column (GE Healthcare) according to manufacturer's instruction. Proteins were eluted with Tris glycerol buffer (50 mM Tris pH 8, 100 mM NaCl, 10% glycerol) and separated into 8 fractions. 1 ml of each fraction (8 ml) was concentrated to 0.1 ml using Amicon Ultra-4 PL-10 centrifugal filter (Millipore) according to manufacturer's instruction. Each 2 of the 8 fractions were then combined together to generate the A, B, C and D pools. All the pools were subjected to in vitro acetylation by San in the presence of ATP, resolved by SDS-PAGE, and exposed to phosphor image screen.

3.3 Results

The autoacetylation of San is blocked by soluble proteins

To test whether San could acetylate its potential substrates in cell lysates, HeLa cell lysate was fractionated to soluble proteins (S100) and insoluble proteins (P100) by centrifugation at 100,000g and each fraction was incubated with recombinant San in the presence of ^{14}C-acetyl-CoA. Proteins were separated by SDS-PAGE and acetylation was detected by phosphor image. As shown in Fig. 3.1A, multiple bands were labeled with ^{14}C by San in P100 (right panel, lane 4) but not S100 (right panel, lane 2). Interestingly, compared to the buffer only control (Fig. 3.1A, right panel, lane 5), the autoacetylation of San was reduced in S100 but not P100. To investigate whether the autoacetylation was weakened by proteins in S100, a portion of S100 was heated to 70°C for 5 minutes to denature most of the proteins and incubated with San. Compared to non-treated S100, heat-treated S100 lost its ability to block the autoacetylation of San (Fig. 3.1B), suggesting that this activity is likely mediated by proteins. Taken together, these results suggest that proteins in HeLa S100 block the autoacetylation of San.

Loss of the San autoacetylation in HeLa S100 is not due to deacetylation of San

Given that the autoacetylation of San was blocked by S100, I reasoned that there is a protein counteracting San activity and sought to identify it. Two possibilities could account for this counteraction. One is that the protein is a deacetylase and removes acetylations on San. Alternatively, the protein is an inhibitor of San and loss of the San autoacetylation is due to inhibition of San activity. To investigate whether San was

deacetylated by proteins in S100, recombinant San was incubated with ^{14}C-acetyl-CoA to allow autoacetylation, followed by incubation with HeLa S100 for indicated time. While S100 blocked the autoacetylation of untreated San as expected (Fig. 3.2, lane 1), the pre-catalyzed autoacetylation on San was not reduced by incubation with S100 (Fig. 3.2, lane 3-4), suggesting that the protein counteracting San activity is not a deacetylase and more likely is a San inhibitor.

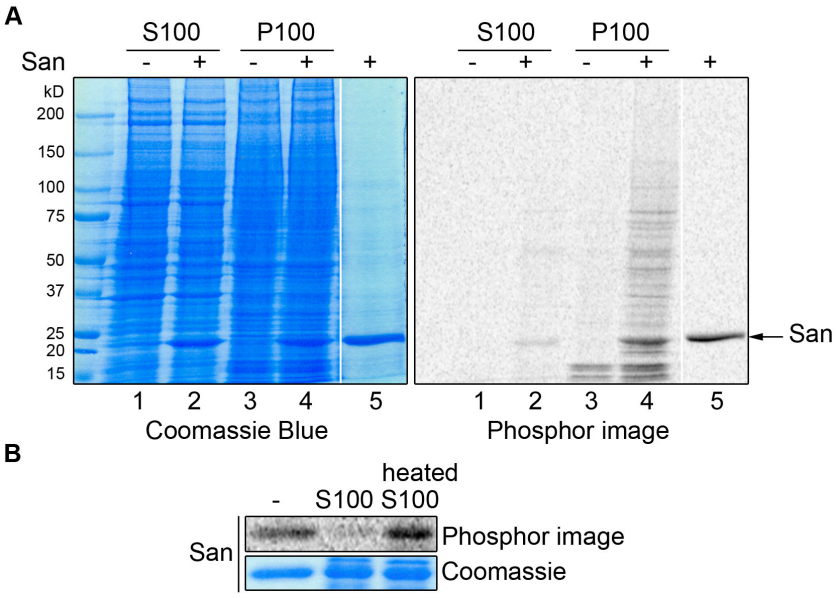

Figure 3.1. Autoacetylation of San is diminished by proteins in HeLa S100.

A. San-catalyzed acetylations in cell lysates. HeLa cell lysates were centrifugally fractionated into soluble (S100) and insoluble (P100) fractions, which were then subjected to the in vitro acetylation assay in the presence or absence of San. Proteins were resolved by SDS-PAGE and analyzed by Coomassie Blue staining (left) and phosphor image (right). **B.** Autoacetylation of San was not affected by heat-denatured HeLa S100. HeLa S100 untreated or denatured by heat was subjected to autoacetylation assay of San.

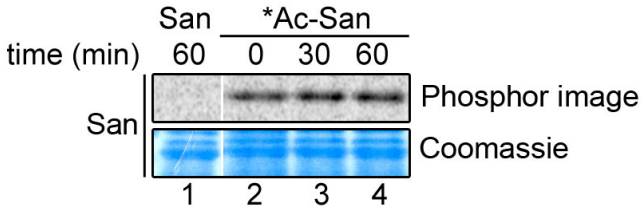

Figure 3.2. San is not deacetylated by proteins in HeLa S100.

Recombinant San was ^{14}C-labeled by autoacetylation with ^{14}C-acetyl CoA and incubated with HeLa S100 for indicated time. As the positive control for the activity of HeLa S100, unlabeled San was incubated with HeLa S100 and ^{14}C-acetyl CoA for 60 minutes (lane 1).

The activity of the San inhibitor requires ATP but not ATP hydrolysis

Having demonstrated that proteins in HeLa S100 were necessary for the inhibition of San activity (Fig. 3.1B), I next asked whether proteins alone are sufficient for the inhibition. Since S100 contains soluble cellular cofactors, it is possible that they are also involved in the inhibition of San. To test this hypothesis, HeLa S100 was applied to desalting columns to separate the protein fraction (P) from the small molecule fraction (SM). The P fraction by itself did not inhibit San autoacetylation (Fig. 3.3A, lane 4), nor did the SM fraction (Fig. 3.3A, lane 7). The inhibition was restored by mixing these two fractions together (Fig. 3.3A, lane 3), suggesting that both proteins and small molecules are necessary. To find out the necessary small molecule, I next mixed the P fraction with different cellular cofactors and found that ATP, but not GTP, could substitute for the SM fraction (Fig. 3.3A, lane 5-6). This result suggests that San activity is inhibited in an ATP-dependent manner.

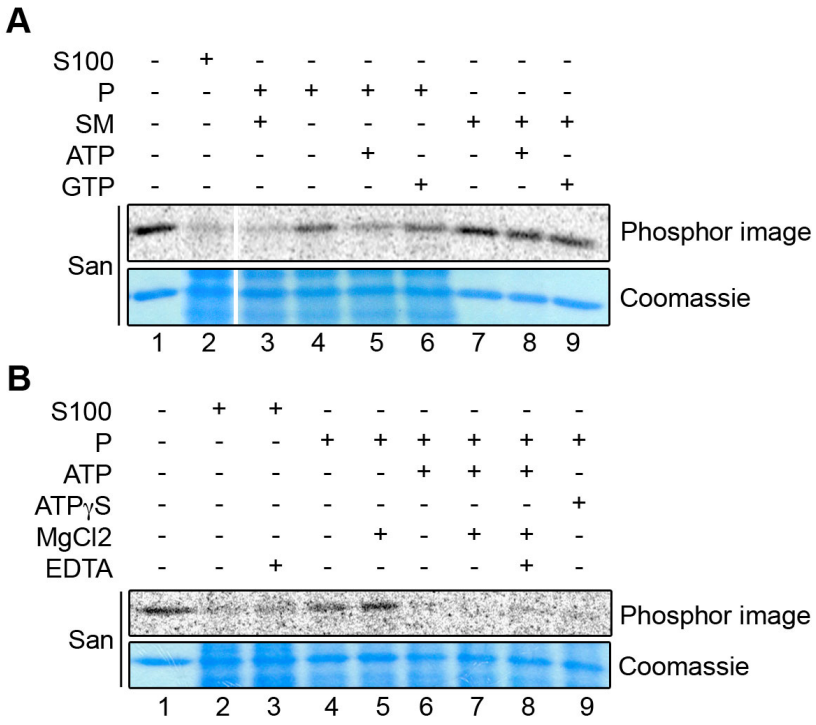

Figure 3.3. ATP but not ATP hydrolysis is required for proteins in HeLa S100 to inhibit San activity.

A. Proteins and ATP were both necessary for the inhibition of San. HeLa S100 was fractionated into protein (P) and small molecule (SM) fractions by desalting column. Autoacetylation assay of San was performed in the presence of ^{14}C-acetyl CoA and indicated components. **B.** ATP hydrolysis was not necessary for the inhibition of San. HeLa S100 was fractionated as in **A** and subjected to autoacetylation assay of San with indicated components.

Next I examined whether ATP hydrolysis is necessary for inhibiting San activity. Magnesium ion is thought to be a catalyst for ATP hydrolysis (Senior, 1979). If ATP hydrolysis is required, removal of magnesium ion by chelating agent EDTA will abolish the inhibitory effect of S100. As shown in Fig. 3.3B, EDTA did not attenuate S100 to inhibit San activity (lane 2-3), and magnesium ion was dispensable for the inhibition

restored by mixing the P fraction and ATP (lane 6-8), both suggesting that magnesium ion is not required for the inhibition. Moreover, ATPγS, a non-hydrolysable ATP analog, could substitute for ATP to restore the inhibition in the P fraction (Fig. 3.3B, lane 9). Taken together, these results indicate that ATP hydrolysis is not required for the San inhibitor.

Partial purification of the inhibitory activity on San

To better understand how San activity is regulated in vivo, I attempted to purify the San inhibitor from HeLa S100. I first increased its protein concentration by ammonium sulfate fractionation. Saturated ammonium sulfate solution was added to HeLa S100 at a final concentration as indicated, and precipitated proteins were resuspended to a similar concentration as in S100, desalted, and incubated with San and ^{14}C-acetyl-CoA in the presence or absence of ATP. As shown in Fig. 3.4A, the ATP-dependent San inhibitor was enriched in the 40-100% fraction (lane 7-8). To test whether the San inhibitor could be purified by its affinity to ATP, the 40-100% fraction was incubated with ATP-conjugated resin, and proteins bound to the resin were eluted by 20 mM ATP for three times. Three eluants (E1, E2, E3) as well as the input lysate (I) were incubated with San and ^{14}C-acetyl-CoA in the presence or absence of ATP. As shown in Fig. 3.4B, I, E2 and E3 exhibited partial inhibition of San activity (lane3-7). After decreasing the concentration of San proteins to 50 ng/ml, the inhibitory activity in E2 and E3 were more prominent (Fig. 3.4B, lane 10-11), suggesting that the concentration of the San inhibitor in E2 and E3 were at least two fold lower than that in HeLa S100. This dilution effect may be due to inefficient pulldown of the inhibitor from the lysate or

inefficient elution of the inhibitor from the resin. This result indicates that the San inhibitor can be purified by its affinity to ATP, and further optimization of the purification procedure is required for better yield.

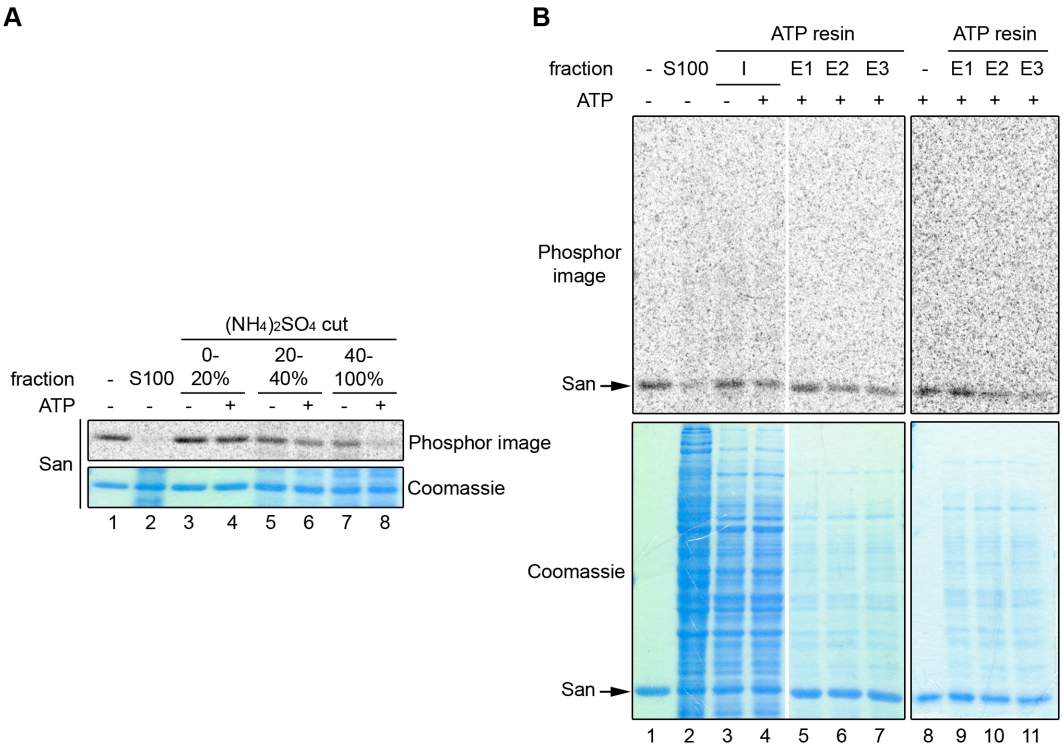

Figure 3.4. Partial purification of the San inhibitor by ammonium sulfate fractionation and ATP-conjugated resin.

A. Ammonium sulfate fractionation of HeLa S100. HeLa S100 was fractionated into 3 fractions by indicated concentrations of ammonium sulfate. All fractions were desalted and subjected to autoacetylation assay of San in the presence or absence of ATP. **B**. Purification of the San inhibitor by its affinity to ATP. HeLa S100 was fractionated as in **A**, and the 40-100% fraction (I) was incubated with ATP-conjugated resin. Proteins bound to the resin were eluted by free ATP for 3 times, and all the eluants were subjected to autoacetylation assay of San in the presence or absence of ATP. Samples in lane 8-11 were the same assay as those in lane 1 and 5-7 but used only half amount of San.

In addition to affinity purification, I also tested whether gel filtration chromatography helps to isolate the San inhibitor. The 40-100% ammonium sulfate fraction of HeLa S100 was applied to a Superdex 200 column, separated into eight fractions, and the proteins were concentrated to the same volume as that of the input lysate. Each fraction was then incubated with San and ^{14}C-acetyl-CoA in the presence of ATP. However, none of the fraction inhibited San while mixing the 8 fractions together restored the inhibition. I reasoned that the San inhibitor might be a multi-subunit protein complex and the complex was dissociated during the gel filtration process. To find out which fractions contained the components of the San inhibitor, each two of the eight fractions were combined to generate four pools (Fig. 3.5A). Each pool were mixed with either buffer or other fractions and incubated with San and ^{14}C-acetyl-CoA. As shown in Fig. 3.5B, none of the four pools alone inhibited San (lane 7-10), nor did the combinations of any two of them (data not shown). Combination of the A, B and C pools partially restored the inhibition (Fig. 3.5B, lane 11), suggesting that components of the San inhibitor were distributed into a wide range of fractions after gel filtration chromatography. More experiments are necessary to dissect the distribution of the inhibitor in these fractions (see below).

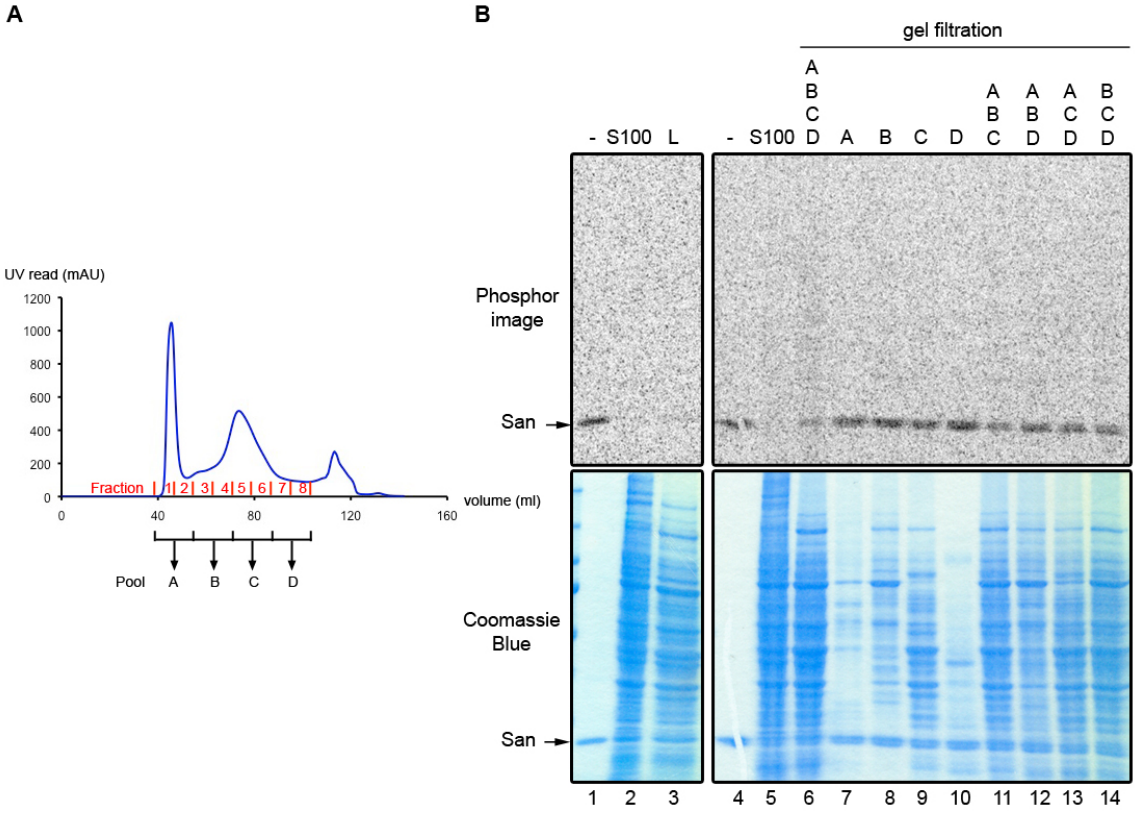

Figure 3.5. Partial purification of the San inhibitor by gel filtration chromatography.

HeLa S100 was fractionated by ammonium sulfate fractionation, and the 40-100% fraction (L) was passed through the Superdex 200 column. **A.** Chromograph of the purification. 8 fractions were collected, concentrated, and combined into 4 pools (A-D). **B.** All the pools, by itself or combined with others, were subjected to autoacetylation assay of San in the presence of ATP.

3.4 Summary and future plan

Here I show that the lysine acetyltransferase activity of San is inhibited by a protein complex in an ATP-dependent manner. However, the fact that ATP hydrolysis is not necessary suggests that this inhibition is not achieved by phosphorylation or energy-consuming processes. It is possible that ATP binding to the San inhibitor induces conformational changes required for its association with San and the association is sufficient to inhibit San activity.

The San inhibitor was partially purified by ATP affinity binding and gel filtration chromatography. The inhibitory activity could only be reconstituted by combining multiple fractions (Fig. 3.5), suggesting that this inhibitor is a protein complex and is dissociated under this chromatography condition. Ion exchange chromatography will be an alternate way to purify the inhibitor if its activity sustains high salt concentration. In the case that ion exchange is not suitable, hydrophobic interaction chromatography or gel filtration chromatography with a higher resolution will be considered. The presence of ATP throughout the whole process may stabilize the inhibitor. By combining different fractions to reconstitute the inhibitory activity, fractions containing the components of the inhibitor will be mapped out and those components will be identified by mass spectrometry. ATP affinity purification can follow the chromatography to further enrich the inhibitor if necessary.

CHAPTER FOUR

CONCLUSION AND FUTURE DIRECTIONS

San is an acetyltransferase required for sister chromatid cohesion, and its functions are essential in *Drosophila*. To better understand how San functions and how its activity is regulated in the cell, I searched for its downstream effector and upstream regulator. In this dissertation, I demonstrated that San is a tubulin acetyltransferase that targets β-tubulin K252 on tubulin heterodimers. Mutants mimicking K252-acetylated tubulin are incorporated into MTs in a much slower rate, and depletion of San accelerates the rate of MT regrowth after cold-induced catastrophe, together suggesting that San inhibits tubulin polymerization by acetylating β-tubulin K252. I also presented evidence indicating the existence of a San inhibitor, which inhibits San in an ATP-dependent but hydrolysis-independent manner. Although the identity of the inhibitor remains undetermined, gel filtration chromatography analysis suggests that it may be a protein complex.

MTs are key components of the cytoskeleton and play critical roles in numerous cellular events. Posttranslational modifications on tubulin diversify MTs to fulfill different functions. While most modifications are found on MTs and regulate the association between MT and MAPs, acetylation on β-tubulin K252 as well as phosphorylation on β-tubulin S172 occur on free tubulins and regulate tubulin incorporation into MTs (Fourest-Lieuvin et al., 2006; Westermann and Weber, 2003).

Interestingly, K252 and S172 locate in proximity to the α-tubulin-bound GTP and β-tubulin-bound GTP respectively, raising the possibility that both modifications regulate tubulin polymerization by affecting the interaction between GTP and surrounding microenvironment. As a result, acetylation on K252 may weaken the intradimer interaction, whereas phosphorylation on S172 may weaken the association between GTP and β-tubulin.

Another feature of K252 is that it is not conserved in α-tubulin, which harbors a glutamic acid at this position. Generally residues surrounding the nucleotide binding site are conserved between α- and β-tubulin, but there are exceptions, with position 252 (254 in α-tubulin) the most significant one among them. While K252 in β-tubulin is proposed to interact and stabilize the α-tubulin-bound GTP, E254 in α-tubulin is thought to facilitate the hydrolysis of the β-tubulin-bound GTP (Lowe et al., 2001). A α-tubulin mutation impeding GTP incorporation and subsequent heterodimer formation has been shown to impair neuronal migration (Keays et al., 2007). Therefore it would be of great interest to investigate whether K252 acetylation affects the incorporation or hydrolysis of the α-tubulin-bound GTP, which is normally non-hydrolysable.

In addition to weakening the interaction between the α-tubulin-bound GTP and β-tubulin, acetylation on K252 may cause conformational changes within β-tubulin, most likely the colchicine binding site. The K252-containing peptide 247-265 is part of the binding site and involved in taxol-induced MT stabilization (Xiao et al., 2006). Point mutations within or close to this region have been shown responsible for the resistance to 2ME2 in cancer cells (Gokmen-Polar et al., 2005; Liaw et al., 2008). 2ME2 is another

MT-depolymerizing drug binding to the colchicine binding site. These studies suggest that mutations within this region may alter tubulin conformation and affect MT stability, which may also occur when K252 is acetylated. Taken together, the effect of the K252 acetylation on tubulin polymerization may result from the combination of weakened intradimer interaction and altered tubulin conformation.

Unlike most modifications, the K252 acetylation occurs on tubulins and directly affects MT assembly. Although the effect on gross MT organization seems relatively weak in HeLa cells, it is possible that the physiological significance of this acetylation is more noticeable in neuronal cells, which heavily rely on MTs for their specialized cellular functions. Further studies using animal models are required to reveal the regulatory mechanism of this acetylation, which is critical to elucidate its exact biological significance.

Lysine acetylation is crucial for modulating numerous cellular events; hence the activity of acetyltransferase has to be fine-tuned. San catalyzes both N-terminal acetylation and lysine acetylation, and its activity is required for centromeric cohesion, chromosome resolution, and MT dynamics (Hou et al., 2007; Pimenta-Marques et al., 2008; Williams et al., 2003). Therefore, it is worthwhile to further investigate how San functions are regulated in vivo. Since the protein level or localization of San remains unchanged during cell cycle progression, it is important that its activity and substrate specificity are tightly controlled (Hou et al., 2007). Several mechanisms may contribute to the regulation of San. Similar to other lysine acetyltransferases, the autoacetylation of San acts as a switch of its enzymatic activity (Evjenth et al., 2009). In addition, proteomic studies revealed that San is phosphorylated at multiple sites (Dephoure et al., 2008; Rush

et al., 2005). These phosphorylations may be part of the regulatory mechanism for San as seen for other acetyltransferases. Moreover, San is part of the NatA complex, which may affect San's N-acetyltransferase activity or even its lysine acetyltransferase activity (Hou et al., 2007). Furthermore, my findings suggest that the lysine acetyltransferase activity of San is inhibited by a protein in an ATP-dependent manner. Taken together, it seems that there are multiple mechanisms regulating the enzymatic activity of San, and further studies on the San inhibitor will help elucidate this regulation network.

Another intriguing question about San is its subcellular localization. Given that San is small enough to diffuse through the nuclear pore but remains in the cytoplasm (Mattaj and Englmeier, 1998), San must be excluded from the nucleus by nuclear export mechanisms or binding to other cytoplasmic proteins. For now I did not find any known nuclear export signal within San. Therefore, the localization of San is likely regulated by its binding partners. It would be of great interest to investigate how the spatial distribution of San is regulated.

BIBLIOGRAPHY

Akhmanova, A., and M.O. Steinmetz. 2008. Tracking the ends: a dynamic protein network controls the fate of microtubule tips. *Nat Rev Mol Cell Biol*. 9:309-22.

Al-Bassam, J., R.S. Ozer, D. Safer, S. Halpain, and R.A. Milligan. 2002. MAP2 and tau bind longitudinally along the outer ridges of microtubule protofilaments. *J Cell Biol*. 157:1187-96.

Arnal, I., C. Heichette, G.S. Diamantopoulos, and D. Chretien. 2004. CLIP-170/tubulin-curved oligomers coassemble at microtubule ends and promote rescues. *Curr Biol*. 14:2086-95.

Arnesen, T., D. Anderson, J. Torsvik, H.B. Halseth, J.E. Varhaug, and J.R. Lillehaug. 2006. Cloning and characterization of hNAT5/hSAN: an evolutionarily conserved component of the NatA protein N-alpha-acetyltransferase complex. *Gene*. 371:291-5.

Audebert, S., E. Desbruyeres, C. Gruszczynski, A. Koulakoff, F. Gros, P. Denoulet, and B. Edde. 1993. Reversible polyglutamylation of alpha- and beta-tubulin and microtubule dynamics in mouse brain neurons. *Mol Biol Cell*. 4:615-26.

Baker, S.P., and P.A. Grant. 2007. The SAGA continues: expanding the cellular role of a transcriptional co-activator complex. *Oncogene*. 26:5329-40.

Belmont, L.D., and T.J. Mitchison. 1996. Identification of a protein that interacts with tubulin dimers and increases the catastrophe rate of microtubules. *Cell*. 84:623-31.

Bieling, P., S. Kandels-Lewis, I.A. Telley, J. van Dijk, C. Janke, and T. Surrey. 2008. CLIP-170 tracks growing microtubule ends by dynamically recognizing composite EB1/tubulin-binding sites. *J Cell Biol*. 183:1223-33.

Bieling, P., L. Laan, H. Schek, E.L. Munteanu, L. Sandblad, M. Dogterom, D. Brunner, and T. Surrey. 2007. Reconstitution of a microtubule plus-end tracking system in vitro. *Nature*. 450:1100-5.

Blanco-Garcia, N., E. Asensio-Juan, X. de la Cruz, and M.A. Martinez-Balbas. 2009. Autoacetylation regulates P/CAF nuclear localization. *J Biol Chem*. 284:1343-52.

Bobinnec, Y., M. Moudjou, J.P. Fouquet, E. Desbruyeres, B. Edde, and M. Bornens. 1998. Glutamylation of centriole and cytoplasmic tubulin in proliferating non-neuronal cells. *Cell Motil Cytoskeleton*. 39:223-32.

Boucher, D., J.C. Larcher, F. Gros, and P. Denoulet. 1994. Polyglutamylation of tubulin as a progressive regulator of in vitro interactions between the microtubule-associated protein Tau and tubulin. *Biochemistry*. 33:12471-7.

Bouras, T., M. Fu, A.A. Sauve, F. Wang, A.A. Quong, N.D. Perkins, R.T. Hay, W. Gu, and R.G. Pestell. 2005. SIRT1 deacetylation and repression of p300 involves lysine residues 1020/1024 within the cell cycle regulatory domain 1. *J Biol Chem*. 280:10264-76.

Bre, M.H., V. Redeker, M. Quibell, J. Darmanaden-Delorme, C. Bressac, J. Cosson, P. Huitorel, J.M. Schmitter, J. Rossler, T. Johnson, A. Adoutte, and N. Levilliers. 1996. Axonemal tubulin polyglycylation probed with two monoclonal antibodies: widespread evolutionary distribution, appearance during spermatozoan maturation and possible function in motility. *J Cell Sci*. 109 (Pt 4):727-38.

Brouhard, G.J., J.H. Stear, T.L. Noetzel, J. Al-Bassam, K. Kinoshita, S.C. Harrison, J. Howard, and A.A. Hyman. 2008. XMAP215 is a processive microtubule polymerase. *Cell*. 132:79-88.

Brownell, J.E., and C.D. Allis. 1995. An activity gel assay detects a single, catalytically active histone acetyltransferase subunit in Tetrahymena macronuclei. *Proc Natl Acad Sci U S A*. 92:6364-8.

Brownell, J.E., and C.D. Allis. 1996. Special HATs for special occasions: linking histone acetylation to chromatin assembly and gene activation. *Curr Opin Genet Dev*. 6:176-84.

Caplow, M., R.L. Ruhlen, and J. Shanks. 1994. The free energy for hydrolysis of a microtubule-bound nucleotide triphosphate is near zero: all of the free energy for hydrolysis is stored in the microtubule lattice. *J Cell Biol*. 127:779-88.

Casanova, M., L. Crobu, C. Blaineau, N. Bourgeois, P. Bastien, and M. Pages. 2009. Microtubule-severing proteins are involved in flagellar length control and mitosis in Trypanosomatids. *Mol Microbiol*. 71:1353-70.

Cassimeris, L. 2002. The oncoprotein 18/stathmin family of microtubule destabilizers. *Curr Opin Cell Biol*. 14:18-24.

Cassimeris, L., D. Gard, P.T. Tran, and H.P. Erickson. 2001. XMAP215 is a long thin molecule that does not increase microtubule stiffness. *J Cell Sci*. 114:3025-33.

Caviston, J.P., and E.L. Holzbaur. 2006. Microtubule motors at the intersection of trafficking and transport. *Trends Cell Biol*. 16:530-7.

Choudhary, C., C. Kumar, F. Gnad, M.L. Nielsen, M. Rehman, T.C. Walther, J.V. Olsen, and M. Mann. 2009. Lysine acetylation targets protein complexes and co-regulates major cellular functions. *Science*. 325:834-40.

Chretien, D., S.D. Fuller, and E. Karsenti. 1995. Structure of growing microtubule ends: two-dimensional sheets close into tubes at variable rates. *J Cell Biol*. 129:1311-28.

Creppe, C., L. Malinouskaya, M.-L. Volvert, M. Gillard, P. Close, O. Malaise, S. Laguesse, I. Cornez, S. Rahmouni, S. Ormenese, S. Belachew, B. Malgrange, J.-P. Chapelle, U. Siebenlist, G. Moonen, A. Chariot, and L. Nguyen. 2009. Elongator Controls the Migration and Differentiation of Cortical Neurons through Acetylation of [alpha]-Tubulin. *Cell*. 136:551-564.

Curmi, P.A., S.S. Andersen, S. Lachkar, O. Gavet, E. Karsenti, M. Knossow, and A. Sobel. 1997. The stathmin/tubulin interaction in vitro. *J Biol Chem*. 272:25029-36.

Dai, J., A.V. Kateneva, and J.M. Higgins. 2009. Studies of haspin-depleted cells reveal that spindle-pole integrity in mitosis requires chromosome cohesion. *J Cell Sci*. 122:4168-76.

Davenport, J.R., A.J. Watts, V.C. Roper, M.J. Croyle, T. van Groen, J.M. Wyss, T.R. Nagy, R.A. Kesterson, and B.K. Yoder. 2007. Disruption of intraflagellar transport in adult mice leads to obesity and slow-onset cystic kidney disease. *Curr Biol*. 17:1586-94.

Davies, J., and G.D. Wright. 1997. Bacterial resistance to aminoglycoside antibiotics. *Trends Microbiol*. 5:234-40.

Dehmelt, L., and S. Halpain. 2005. The MAP2/Tau family of microtubule-associated proteins. *Genome Biol*. 6:204.

Dephoure, N., C. Zhou, J. Villen, S.A. Beausoleil, C.E. Bakalarski, S.J. Elledge, and S.P. Gygi. 2008. A quantitative atlas of mitotic phosphorylation. *Proc Natl Acad Sci U S A*. 105:10762-7.

Dimitrov, A., M. Quesnoit, S. Moutel, I. Cantaloube, C. Pous, and F. Perez. 2008. Detection of GTP-tubulin conformation in vivo reveals a role for GTP remnants in microtubule rescues. *Science*. 322:1353-6.

Dixit, R., B. Barnett, J.E. Lazarus, M. Tokito, Y.E. Goldman, and E.L. Holzbaur. 2009. Microtubule plus-end tracking by CLIP-170 requires EB1. *Proc Natl Acad Sci U S A*. 106:492-7.

Dixit, R., J.L. Ross, Y.E. Goldman, and E.L. Holzbaur. 2008. Differential regulation of dynein and kinesin motor proteins by tau. *Science*. 319:1086-9.

Dompierre, J.P., J.D. Godin, B.C. Charrin, F.P. Cordelieres, S.J. King, S. Humbert, and F. Saudou. 2007. Histone Deacetylase 6 Inhibition Compensates for the Transport Deficit in Huntington's Disease by Increasing Tubulin Acetylation. *J. Neurosci.* 27:3571-3583.

Dunn, S., E.E. Morrison, T.B. Liverpool, C. Molina-Paris, R.A. Cross, M.C. Alonso, and M. Peckham. 2008. Differential trafficking of Kif5c on tyrosinated and detyrosinated microtubules in live cells. *J Cell Sci*. 121:1085-95.

Edde, B., J. Rossier, J.P. Le Caer, E. Desbruyeres, F. Gros, and P. Denoulet. 1990. Posttranslational glutamylation of alpha-tubulin. *Science*. 247:83-5.

Elie-Caille, C., F. Severin, J. Helenius, J. Howard, D.J. Muller, and A.A. Hyman. 2007. Straight GDP-tubulin protofilaments form in the presence of taxol. *Curr Biol*. 17:1765-70.

Erck, C., L. Peris, A. Andrieux, C. Meissirel, A.D. Gruber, M. Vernet, A. Schweitzer, Y. Saoudi, H. Pointu, C. Bosc, P.A. Salin, D. Job, and J. Wehland. 2005. A vital role of tubulin-tyrosine-ligase for neuronal organization. *Proc Natl Acad Sci U S A*. 102:7853-8.

Ersfeld, K., J. Wehland, U. Plessmann, H. Dodemont, V. Gerke, and K. Weber. 1993. Characterization of the tubulin-tyrosine ligase. *J Cell Biol*. 120:725-32.

Evjenth, R., K. Hole, O.A. Karlsen, M. Ziegler, T. Arnesen, and J.R. Lillehaug. 2009. Human Naa50p (Nat5/San) displays both protein N alpha- and N epsilon-acetyltransferase activity. *J Biol Chem*. 284:31122-9.

Faiola, F., X. Liu, S. Lo, S. Pan, K. Zhang, E. Lymar, A. Farina, and E. Martinez. 2005. Dual regulation of c-Myc by p300 via acetylation-dependent control of Myc protein turnover and coactivation of Myc-induced transcription. *Mol Cell Biol*. 25:10220-34.

Fourest-Lieuvin, A., L. Peris, V. Gache, I. Garcia-Saez, C. Juillan-Binard, V. Lantez, and D. Job. 2006. Microtubule regulation in mitosis: tubulin phosphorylation by the cyclin-dependent kinase Cdk1. *Mol Biol Cell*. 17:1041-50.

Frickey, T., and A.N. Lupas. 2004. Phylogenetic analysis of AAA proteins. *J Struct Biol*. 146:2-10.

Fukushige, T., Z.K. Siddiqui, M. Chou, J.G. Culotti, C.B. Gogonea, S.S. Siddiqui, and M. Hamelin. 1999. MEC-12, an alpha-tubulin required for touch sensitivity in C. elegans. *J Cell Sci*. 112 (Pt 3):395-403.

Fukushima, N., D. Furuta, Y. Hidaka, R. Moriyama, and T. Tsujiuchi. 2009. Post-translational modifications of tubulin in the nervous system. *J Neurochem*. 109:683-93.

Gaitanos, T.N., R.M. Buey, J.F. Diaz, P.T. Northcote, P. Teesdale-Spittle, J.M. Andreu, and J.H. Miller. 2004. Peloruside A does not bind to the taxoid site on beta-tubulin and retains its activity in multidrug-resistant cell lines. *Cancer Res*. 64:5063-7.

Gamblin, T.C., K. Nachmanoff, S. Halpain, and R.C. Williams, Jr. 1996. Recombinant microtubule-associated protein 2c reduces the dynamic instability of individual microtubules. *Biochemistry*. 35:12576-86.

Gautschi, M., S. Just, A. Mun, S. Ross, P. Rucknagel, Y. Dubaquie, A. Ehrenhofer-Murray, and S. Rospert. 2003. The yeast N(alpha)-acetyltransferase NatA is quantitatively anchored to the ribosome and interacts with nascent polypeptides. *Mol Cell Biol*. 23:7403-14.

Gigant, B., P.A. Curmi, C. Martin-Barbey, E. Charbaut, S. Lachkar, L. Lebeau, S. Siavoshian, A. Sobel, and M. Knossow. 2000. The 4 A X-ray structure of a tubulin:stathmin-like domain complex. *Cell*. 102:809-16.

Gigant, B., C. Wang, R.B. Ravelli, F. Roussi, M.O. Steinmetz, P.A. Curmi, A. Sobel, and M. Knossow. 2005. Structural basis for the regulation of tubulin by vinblastine. *Nature*. 435:519-22.

Gokmen-Polar, Y., D. Escuin, C.D. Walls, S.E. Soule, Y. Wang, K.L. Sanders, T.M. Lavallee, M. Wang, B.D. Guenther, P. Giannakakou, and G.W. Sledge, Jr. 2005. beta-Tubulin mutations are associated with resistance to 2-methoxyestradiol in MDA-MB-435 cancer cells. *Cancer Res*. 65:9406-14.

Goshima, G., R. Wollman, N. Stuurman, J.M. Scholey, and R.D. Vale. 2005. Length control of the metaphase spindle. *Curr Biol*. 15:1979-88.

Guelman, S., K. Kozuka, Y. Mao, V. Pham, M.J. Solloway, J. Wang, J. Wu, J.R. Lill, and J. Zha. 2009. The double-histone-acetyltransferase complex ATAC is essential for mammalian development. *Mol Cell Biol*. 29:1176-88.

Gundersen, G.G., S. Khawaja, and J.C. Bulinski. 1987. Postpolymerization detyrosination of alpha-tubulin: a mechanism for subcellular differentiation of microtubules. *J Cell Biol*. 105:251-64.

Gupta, M.L., Jr., P. Carvalho, D.M. Roof, and D. Pellman. 2006. Plus end-specific depolymerase activity of Kip3, a kinesin-8 protein, explains its role in positioning the yeast mitotic spindle. *Nat Cell Biol*. 8:913-23.

Helenius, J., G. Brouhard, Y. Kalaidzidis, S. Diez, and J. Howard. 2006. The depolymerizing kinesin MCAK uses lattice diffusion to rapidly target microtubule ends. *Nature*. 441:115-9.

Hertzer, K.M., and C.E. Walczak. 2008. The C-termini of tubulin and the specific geometry of tubulin substrates influence the depolymerization activity of MCAK. *Cell Cycle*. 7:2727-37.

Hickman, A.B., M.A. Namboodiri, D.C. Klein, and F. Dyda. 1999. The structural basis of ordered substrate binding by serotonin N-acetyltransferase: enzyme complex at 1.8 A resolution with a bisubstrate analog. *Cell*. 97:361-9.

Hoebeke, J., G. Van Nijen, and M. De Brabander. 1976. Interaction of oncodazole (R 17934), a new antitumoral drug, with rat brain tubulin. *Biochem Biophys Res Commun*. 69:319-24.

Holmfeldt, P., M.E. Sellin, and M. Gullberg. 2009. Predominant regulators of tubulin monomer-polymer partitioning and their implication for cell polarization. *Cell Mol Life Sci*. 66:3263-76.

Honnappa, S., S.M. Gouveia, A. Weisbrich, F.F. Damberger, N.S. Bhavesh, H. Jawhari, I. Grigoriev, F.J. van Rijssel, R.M. Buey, A. Lawera, I. Jelesarov, F.K. Winkler, K. Wuthrich, A. Akhmanova, and M.O. Steinmetz. 2009. An EB1-binding motif acts as a microtubule tip localization signal. *Cell*. 138:366-76.

Hou, F., C.W. Chu, X. Kong, K. Yokomori, and H. Zou. 2007. The acetyltransferase activity of San stabilizes the mitotic cohesin at the centromeres in a shugoshin-independent manner. *J Cell Biol*. 177:587-97.

Hou, F., and H. Zou. 2005. Two human orthologues of Eco1/Ctf7 acetyltransferases are both required for proper sister-chromatid cohesion. *Mol Biol Cell*. 16:3908-18.

Howell, B., N. Larsson, M. Gullberg, and L. Cassimeris. 1999. Dissociation of the tubulin-sequestering and microtubule catastrophe-promoting activities of oncoprotein 18/stathmin. *Mol Biol Cell*. 10:105-18.

Hubbert, C., A. Guardiola, R. Shao, Y. Kawaguchi, A. Ito, A. Nixon, M. Yoshida, X.F. Wang, and T.P. Yao. 2002. HDAC6 is a microtubule-associated deacetylase. *Nature*. 417:455-8.

Hunter, A.W., M. Caplow, D.L. Coy, W.O. Hancock, S. Diez, L. Wordeman, and J. Howard. 2003. The kinesin-related protein MCAK is a microtubule depolymerase that forms an ATP-hydrolyzing complex at microtubule ends. *Mol Cell*. 11:445-57.

Huzil, J.T., J.K. Chik, G.W. Slysz, H. Freedman, J. Tuszynski, R.E. Taylor, D.L. Sackett, and D.C. Schriemer. 2008. A unique mode of microtubule stabilization induced by peloruside A. *J Mol Biol*. 378:1016-30.

Hyman, A.A., S. Salser, D.N. Drechsel, N. Unwin, and T.J. Mitchison. 1992. Role of GTP hydrolysis in microtubule dynamics: information from a slowly hydrolyzable analogue, GMPCPP. *Mol Biol Cell*. 3:1155-67.

Ikegami, K., R.L. Heier, M. Taruishi, H. Takagi, M. Mukai, S. Shimma, S. Taira, K. Hatanaka, N. Morone, I. Yao, P.K. Campbell, S. Yuasa, C. Janke, G.R. Macgregor, and M. Setou. 2007. Loss of alpha-tubulin polyglutamylation in ROSA22 mice is associated with abnormal targeting of KIF1A and modulated synaptic function. *Proc Natl Acad Sci U S A*. 104:3213-8.

Iwata, A., B.E. Riley, J.A. Johnston, and R.R. Kopito. 2005. HDAC6 and microtubules are required for autophagic degradation of aggregated huntingtin. *J Biol Chem*. 280:40282-92.

Janke, C., K. Rogowski, D. Wloga, C. Regnard, A.V. Kajava, J.M. Strub, N. Temurak, J. van Dijk, D. Boucher, A. van Dorsselaer, S. Suryavanshi, J. Gaertig, and B. Edde. 2005. Tubulin polyglutamylase enzymes are members of the TTL domain protein family. *Science*. 308:1758-62.

Jenuwein, T., and C.D. Allis. 2001. Translating the histone code. *Science*. 293:1074-80.

Jeong, J.W., M.K. Bae, M.Y. Ahn, S.H. Kim, T.K. Sohn, M.H. Bae, M.A. Yoo, E.J. Song, K.J. Lee, and K.W. Kim. 2002. Regulation and destabilization of HIF-1alpha by ARD1-mediated acetylation. *Cell*. 111:709-20.

Jimenez-Barbero, J., A. Canales, P.T. Northcote, R.M. Buey, J.M. Andreu, and J.F. Diaz. 2006. NMR determination of the bioactive conformation of peloruside A bound to microtubules. *J Am Chem Soc*. 128:8757-65.

Jourdain, L., P. Curmi, A. Sobel, D. Pantaloni, and M.F. Carlier. 1997. Stathmin: a tubulin-sequestering protein which forms a ternary T2S complex with two tubulin molecules. *Biochemistry*. 36:10817-21.

Kalinina, E., R. Biswas, I. Berezniuk, A. Hermoso, F.X. Aviles, and L.D. Fricker. 2007. A novel subfamily of mouse cytosolic carboxypeptidases. *FASEB J*. 21:836-50.

Kavallaris, M. 2010. Microtubules and resistance to tubulin-binding agents. *Nat Rev Cancer*. 10:194-204.

Kawaguchi, Y., J.J. Kovacs, A. McLaurin, J.M. Vance, A. Ito, and T.P. Yao. 2003. The deacetylase HDAC6 regulates aggresome formation and cell viability in response to misfolded protein stress. *Cell*. 115:727-38.

Keays, D.A., G. Tian, K. Poirier, G.J. Huang, C. Siebold, J. Cleak, P.L. Oliver, M. Fray, R.J. Harvey, Z. Molnar, M.C. Pinon, N. Dear, W. Valdar, S.D. Brown, K.E. Davies, J.N. Rawlins, N.J. Cowan, P. Nolan, J. Chelly, and J. Flint. 2007. Mutations in alpha-tubulin cause abnormal neuronal migration in mice and lissencephaly in humans. *Cell*. 128:45-57.

Kirschner, M., and T. Mitchison. 1986. Beyond self-assembly: from microtubules to morphogenesis. *Cell*. 45:329-42.

Kita, K., T. Wittmann, I.S. Nathke, and C.M. Waterman-Storer. 2006. Adenomatous polyposis coli on microtubule plus ends in cell extensions can promote microtubule net growth with or without EB1. *Mol Biol Cell*. 17:2331-45.

Komarova, Y., C.O. De Groot, I. Grigoriev, S.M. Gouveia, E.L. Munteanu, J.M. Schober, S. Honnappa, R.M. Buey, C.C. Hoogenraad, M. Dogterom, G.G. Borisy, M.O. Steinmetz, and A. Akhmanova. 2009. Mammalian end binding proteins control persistent microtubule growth. *J Cell Biol*. 184:691-706.

Komarova, Y.A., A.S. Akhmanova, S. Kojima, N. Galjart, and G.G. Borisy. 2002. Cytoplasmic linker proteins promote microtubule rescue in vivo. *J Cell Biol*. 159:589-99.

Kreitzer, G., G. Liao, and G.G. Gundersen. 1999. Detyrosination of tubulin regulates the interaction of intermediate filaments with microtubules in vivo via a kinesin-dependent mechanism. *Mol Biol Cell*. 10:1105-18.

LeDizet, M., and G. Piperno. 1987. Identification of an acetylation site of Chlamydomonas alpha-tubulin. *Proc Natl Acad Sci U S A*. 84:5720-4.

Liaw, T.Y., N.K. Salam, M.J. McKay, A.M. Cunningham, D.E. Hibbs, and M. Kavallaris. 2008. Class I beta-tubulin mutations in 2-methoxyestradiol-resistant acute lymphoblastic leukemia cells: implications for drug-target interactions. *Mol Cancer Ther*. 7:3150-9.

Llano-Sotelo, B., E.F. Azucena, Jr., L.P. Kotra, S. Mobashery, and C.S. Chow. 2002. Aminoglycosides modified by resistance enzymes display diminished binding to the bacterial ribosomal aminoacyl-tRNA site. *Chem Biol*. 9:455-63.

Lowe, J., H. Li, K.H. Downing, and E. Nogales. 2001. Refined structure of alpha beta-tubulin at 3.5 A resolution. *J Mol Biol*. 313:1045-57.

Luduena, R.F. 1998. Multiple forms of tubulin: different gene products and covalent modifications. *Int Rev Cytol*. 178:207-75.

Mandelkow, E.M., E. Mandelkow, and R.A. Milligan. 1991. Microtubule dynamics and microtubule caps: a time-resolved cryo-electron microscopy study. *J Cell Biol*. 114:977-91.

Maruta, H., K. Greer, and J.L. Rosenbaum. 1986. The acetylation of alpha-tubulin and its relationship to the assembly and disassembly of microtubules. *J Cell Biol*. 103:571-9.

Matsuyama, A., T. Shimazu, Y. Sumida, A. Saito, Y. Yoshimatsu, D. Seigneurin-Berny, H. Osada, Y. Komatsu, N. Nishino, S. Khochbin, S. Horinouchi, and M. Yoshida. 2002. In vivo destabilization of dynamic microtubules by HDAC6-mediated deacetylation. *Embo J*. 21:6820-31.

Mattaj, I.W., and L. Englmeier. 1998. Nucleocytoplasmic transport: the soluble phase. *Annu Rev Biochem*. 67:265-306.

McKeithan, T.W., and J.L. Rosenbaum. 1981. Multiple forms of tubulin in the cytoskeletal and flagellar microtubules of Polytomella. *J Cell Biol*. 91:352-60.

McNally, F. 2000. Capturing a ring of samurai. *Nat Cell Biol*. 2:E4-7.

McNally, K.P., D. Buster, and F.J. McNally. 2002. Katanin-mediated microtubule severing can be regulated by multiple mechanisms. *Cell Motil Cytoskeleton*. 53:337-49.

Mellert, H.S., and S.B. McMahon. 2009. Biochemical pathways that regulate acetyltransferase and deacetylase activity in mammalian cells. *Trends Biochem Sci*. 34:571-8.

Mimori-Kiyosue, Y., I. Grigoriev, G. Lansbergen, H. Sasaki, C. Matsui, F. Severin, N. Galjart, F. Grosveld, I. Vorobjev, S. Tsukita, and A. Akhmanova. 2005. CLASP1 and CLASP2 bind to EB1 and regulate microtubule plus-end dynamics at the cell cortex. *J Cell Biol*. 168:141-53.

Mio, T., T. Yamada-Okabe, M. Arisawa, and H. Yamada-Okabe. 1999. Saccharomyces cerevisiae GNA1, an essential gene encoding a novel acetyltransferase involved in UDP-N-acetylglucosamine synthesis. *J Biol Chem*. 274:424-9.

Mishima, M., R. Maesaki, M. Kasa, T. Watanabe, M. Fukata, K. Kaibuchi, and T. Hakoshima. 2007. Structural basis for tubulin recognition by cytoplasmic linker protein 170 and its autoinhibition. *Proc Natl Acad Sci U S A*. 104:10346-51.

Mitchison, T., and M. Kirschner. 1984. Dynamic instability of microtubule growth. *Nature*. 312:237-42.

Muller-Reichert, T., D. Chretien, F. Severin, and A.A. Hyman. 1998. Structural changes at microtubule ends accompanying GTP hydrolysis: information from a slowly hydrolyzable analogue of GTP, guanylyl (alpha,beta)methylenediphosphonate. *Proc Natl Acad Sci U S A*. 95:3661-6.

Nagy, Z., and L. Tora. 2007. Distinct GCN5/PCAF-containing complexes function as co-activators and are involved in transcription factor and global histone acetylation. *Oncogene*. 26:5341-57.

Nguyen, L., S. Humbert, F. Saudou, and A. Chariot. 2010. Elongator - an emerging role in neurological disorders. *Trends Mol Med*. 16:1-6.

Nogales, E. 2001. Structural insight into microtubule function. *Annu Rev Biophys Biomol Struct*. 30:397-420.

Nogales, E., and H.W. Wang. 2006. Structural intermediates in microtubule assembly and disassembly: how and why? *Curr Opin Cell Biol*. 18:179-84.

Nogales, E., M. Whittaker, R.A. Milligan, and K.H. Downing. 1999. High-Resolution Model of the Microtubule. *Cell*. 96:79-88.

Nogales, E., S.G. Wolf, and K.H. Downing. 1998. Structure of the alpha beta tubulin dimer by electron crystallography. *Nature*. 391:199-203.

North, B.J., B.L. Marshall, M.T. Borra, J.M. Denu, and E. Verdin. 2003. The human Sir2 ortholog, SIRT2, is an NAD+-dependent tubulin deacetylase. *Mol Cell*. 11:437-44.

Palazzo, A., B. Ackerman, and G.G. Gundersen. 2003. Cell biology: Tubulin acetylation and cell motility. *Nature*. 421:230.

Paturle-Lafanechere, L., B. Edde, P. Denoulet, A. Van Dorsselaer, H. Mazarguil, J.P. Le Caer, J. Wehland, and D. Job. 1991. Characterization of a major brain tubulin variant which cannot be tyrosinated. *Biochemistry*. 30:10523-8.

Pimenta-Marques, A., R. Tostoes, T. Marty, V. Barbosa, R. Lehmann, and R.G. Martinho. 2008. Differential requirements of a mitotic acetyltransferase in somatic and germ line cells. *Dev Biol*. 323:197-206.

Polevoda, B., and F. Sherman. 2003. N-terminal acetyltransferases and sequence requirements for N-terminal acetylation of eukaryotic proteins. *J Mol Biol*. 325:595-622.

Pugacheva, E.N., S.A. Jablonski, T.R. Hartman, E.P. Henske, and E.A. Golemis. 2007. HEF1-dependent Aurora A activation induces disassembly of the primary cilium. *Cell*. 129:1351-63.

Qi, D., J. Larsson, and M. Mannervik. 2004. Drosophila Ada2b is required for viability and normal histone H3 acetylation. *Mol Cell Biol*. 24:8080-9.

Qiu, Y., Y. Zhao, M. Becker, S. John, B.S. Parekh, S. Huang, A. Hendarwanto, E.D. Martinez, Y. Chen, H. Lu, N.L. Adkins, D.A. Stavreva, M. Wiench, P.T. Georgel, R.L. Schiltz, and G.L. Hager. 2006. HDAC1 acetylation is linked to progressive modulation of steroid receptor-induced gene transcription. *Mol Cell*. 22:669-79.

Rausa, F.M., 3rd, D.E. Hughes, and R.H. Costa. 2004. Stability of the hepatocyte nuclear factor 6 transcription factor requires acetylation by the CREB-binding protein coactivator. *J Biol Chem*. 279:43070-6.

Ravelli, R.B.G., B. Gigant, P.A. Curmi, I. Jourdain, S. Lachkar, A. Sobel, and M. Knossow. 2004. Insight into tubulin regulation from a complex with colchicine and a stathmin-like domain. *Nature*. 428:198-202.

Raynaud-Messina, B., and A. Merdes. 2007. Gamma-tubulin complexes and microtubule organization. *Curr Opin Cell Biol*. 19:24-30.

Redeker, V., J.P. Le Caer, J. Rossier, and J.C. Prome. 1991. Structure of the polyglutamyl side chain posttranslationally added to alpha-tubulin. *J Biol Chem*. 266:23461-6.

Redeker, V., N. Levilliers, J.M. Schmitter, J.P. Le Caer, J. Rossier, A. Adoutte, and M.H. Bre. 1994. Polyglycylation of tubulin: a posttranslational modification in axonemal microtubules. *Science*. 266:1688-91.

Redeker, V., N. Levilliers, E. Vinolo, J. Rossier, D. Jaillard, D. Burnette, J. Gaertig, and M.H. Bre. 2005. Mutations of tubulin glycylation sites reveal cross-talk between the C termini of alpha- and beta-tubulin and affect the ciliary matrix in Tetrahymena. *J Biol Chem*. 280:596-606.

Redeker, V., R. Melki, D. Prome, J.P. Le Caer, and J. Rossier. 1992. Structure of tubulin C-terminal domain obtained by subtilisin treatment. The major alpha and beta tubulin isotypes from pig brain are glutamylated. *FEBS Lett*. 313:185-92.

Reed, N.A., D. Cai, T.L. Blasius, G.T. Jih, E. Meyhofer, J. Gaertig, and K.J. Verhey. 2006. Microtubule acetylation promotes kinesin-1 binding and transport. *Curr Biol*. 16:2166-72.

Rice, L.M., E.A. Montabana, and D.A. Agard. 2008. The lattice as allosteric effector: structural studies of alphabeta- and gamma-tubulin clarify the role of GTP in microtubule assembly. *Proc Natl Acad Sci U S A*. 105:5378-83.

Ringhoff, D.N., and L. Cassimeris. 2009. Stathmin regulates centrosomal nucleation of microtubules and tubulin dimer/polymer partitioning. *Mol Biol Cell*. 20:3451-8.

Roll-Mecak, A., and R.D. Vale. 2006. Making more microtubules by severing: a common theme of noncentrosomal microtubule arrays? *J Cell Biol*. 175:849-51.

Roll-Mecak, A., and R.D. Vale. 2008. Structural basis of microtubule severing by the hereditary spastic paraplegia protein spastin. *Nature*. 451:363-7.

Rudiger, M., J. Wehland, and K. Weber. 1994. The carboxy-terminal peptide of detyrosinated alpha tubulin provides a minimal system to study the substrate specificity of tubulin-tyrosine ligase. *Eur J Biochem*. 220:309-20.

Rush, J., A. Moritz, K.A. Lee, A. Guo, V.L. Goss, E.J. Spek, H. Zhang, X.M. Zha, R.D. Polakiewicz, and M.J. Comb. 2005. Immunoaffinity profiling of tyrosine phosphorylation in cancer cells. *Nat Biotechnol*. 23:94-101.

Sandblad, L., K.E. Busch, P. Tittmann, H. Gross, D. Brunner, and A. Hoenger. 2006. The Schizosaccharomyces pombe EB1 homolog Mal3p binds and stabilizes the microtubule lattice seam. *Cell*. 127:1415-24.

Santos-Rosa, H., E. Valls, T. Kouzarides, and M. Martinez-Balbas. 2003. Mechanisms of P/CAF auto-acetylation. *Nucleic Acids Res*. 31:4285-92.

Schwarz, P.M., J.R. Liggins, and R.F. Luduena. 1998. Beta-tubulin isotypes purified from bovine brain have different relative stabilities. *Biochemistry*. 37:4687-92.

Senior, A.E. 1979. Tightly bound magnesium in mitochondrial adenosine triphosphatase from beef heart. *J Biol Chem*. 254:11319-22.

Seve, P., and C. Dumontet. 2008. Is class III beta-tubulin a predictive factor in patients receiving tubulin-binding agents? *Lancet Oncol*. 9:168-75.

Shalizi, A., B. Gaudilliere, Z. Yuan, J. Stegmuller, T. Shirogane, Q. Ge, Y. Tan, B. Schulman, J.W. Harper, and A. Bonni. 2006. A calcium-regulated MEF2 sumoylation switch controls postsynaptic differentiation. *Science*. 311:1012-7.

Sharma, N., J. Bryant, D. Wloga, R. Donaldson, R.C. Davis, M. Jerka-Dziadosz, and J. Gaertig. 2007. Katanin regulates dynamics of microtubules and biogenesis of motile cilia. *J Cell Biol*. 178:1065-79.

Shimazu, T., S. Horinouchi, and M. Yoshida. 2007. Multiple histone deacetylases and the CREB-binding protein regulate pre-mRNA 3'-end processing. *J Biol Chem*. 282:4470-8.

Shirasu-Hiza, M., P. Coughlin, and T. Mitchison. 2003. Identification of XMAP215 as a microtubule-destabilizing factor in Xenopus egg extract by biochemical purification. *J Cell Biol*. 161:349-58.

Siegrist, S.E., and C.Q. Doe. 2007. Microtubule-induced cortical cell polarity. *Genes Dev*. 21:483-96.

Solinger, J.A., R. Paolinelli, H. Kloss, F.B. Scorza, S. Marchesi, U. Sauder, D. Mitsushima, F. Capuani, S.R. Sturzenbaum, and G. Cassata. 2010. The Caenorhabditis elegans Elongator complex regulates neuronal alpha-tubulin acetylation. *PLoS Genet*. 6:e1000820.

Spange, S., T. Wagner, T. Heinzel, and O.H. Kramer. 2009. Acetylation of non-histone proteins modulates cellular signalling at multiple levels. *Int J Biochem Cell Biol*. 41:185-98.

Starheim, K.K., D. Gromyko, R. Velde, J.E. Varhaug, and T. Arnesen. 2009. Composition and biological significance of the human Nalpha-terminal acetyltransferases. *BMC Proc*. 3 Suppl 6:S3.

Steinmetz, M.O., R.A. Kammerer, W. Jahnke, K.N. Goldie, A. Lustig, and J. van Oostrum. 2000. Op18/stathmin caps a kinked protofilament-like tubulin tetramer. *EMBO J*. 19:572-80.

Sterner, D.E., and S.L. Berger. 2000. Acetylation of histones and transcription-related factors. *Microbiol Mol Biol Rev*. 64:435-59.

Sterner, D.E., D. Nathan, A. Reindle, E.S. Johnson, and S.L. Berger. 2006. Sumoylation of the yeast Gcn5 protein. *Biochemistry*. 45:1035-42.

Svejstrup, J.Q. 2007. Elongator complex: how many roles does it play? *Curr Opin Cell Biol*. 19:331-6.

Tanaka, T.U., and A. Desai. 2008. Kinetochore-microtubule interactions: the means to the end. *Curr Opin Cell Biol*. 20:53-63.

Thompson, P.R., D. Wang, L. Wang, M. Fulco, N. Pediconi, D. Zhang, W. An, Q. Ge, R.G. Roeder, J. Wong, M. Levrero, V. Sartorelli, R.J. Cotter, and P.A. Cole. 2004. Regulation of the p300 HAT domain via a novel activation loop. *Nat Struct Mol Biol*. 11:308-15.

Tran, A.D.-A., T.P. Marmo, A.A. Salam, S. Che, E. Finkelstein, R. Kabarriti, H.S. Xenias, R. Mazitschek, C. Hubbert, Y. Kawaguchi, M.P. Sheetz, T.-P. Yao, and J.C. Bulinski. 2007. HDAC6 deacetylation of tubulin modulates dynamics of cellular adhesions. *J Cell Sci*. 120:1469-1479.

Valenzuela-Fernandez, A., J.R. Cabrero, J.M. Serrador, and F. Sanchez-Madrid. 2008. HDAC6: a key regulator of cytoskeleton, cell migration and cell-cell interactions. *Trends Cell Biol*. 18:291-7.

Varga, V., J. Helenius, K. Tanaka, A.A. Hyman, T.U. Tanaka, and J. Howard. 2006. Yeast kinesin-8 depolymerizes microtubules in a length-dependent manner. *Nat Cell Biol*. 8:957-62.

Verhey, K.J., and J. Gaertig. 2007. The tubulin code. *Cell Cycle*. 6:2152-60.

Vervoorts, J., J.M. Luscher-Firzlaff, S. Rottmann, R. Lilischkis, G. Walsemann, K. Dohmann, M. Austen, and B. Luscher. 2003. Stimulation of c-MYC transcriptional activity and acetylation by recruitment of the cofactor CBP. *EMBO Rep*. 4:484-90.

Vetting, M.W., S.d.C. LP, M. Yu, S.S. Hegde, S. Magnet, S.L. Roderick, and J.S. Blanchard. 2005. Structure and functions of the GNAT superfamily of acetyltransferases. *Arch Biochem Biophys*. 433:212-26.

Vitre, B., F.M. Coquelle, C. Heichette, C. Garnier, D. Chretien, and I. Arnal. 2008. EB1 regulates microtubule dynamics and tubulin sheet closure in vitro. *Nat Cell Biol*. 10:415-21.

Wade, R.H. 2009. On and around microtubules: an overview. *Mol Biotechnol*. 43:177-91.

Wang, H.-W., and E. Nogales. 2005. Nucleotide-dependent bending flexibility of tubulin regulates microtubule assembly. *Nature*. 435:911-915.

Wang, Y.L., F. Faiola, M. Xu, S. Pan, and E. Martinez. 2008. Human ATAC Is a GCN5/PCAF-containing acetylase complex with a novel NC2-like histone fold module that interacts with the TATA-binding protein. *J Biol Chem*. 283:33808-15.

Westermann, S., and K. Weber. 2003. Post-translational modifications regulate microtubule function. *Nat Rev Mol Cell Biol*. 4:938-47.

Williams, B.C., C.M. Garrett-Engele, Z. Li, E.V. Williams, E.D. Rosenman, and M.L. Goldberg. 2003. Two putative acetyltransferases, san and deco, are required for establishing sister chromatid cohesion in Drosophila. *Curr Biol*. 13:2025-36.

Xia, L., B. Hai, Y. Gao, D. Burnette, R. Thazhath, J. Duan, M.H. Bre, N. Levilliers, M.A. Gorovsky, and J. Gaertig. 2000. Polyglycylation of tubulin is essential and affects cell motility and division in Tetrahymena thermophila. *J Cell Biol*. 149:1097-106.

Xiao, H., P. Verdier-Pinard, N. Fernandez-Fuentes, B. Burd, R. Angeletti, A. Fiser, S.B. Horwitz, and G.A. Orr. 2006. Insights into the mechanism of microtubule stabilization by Taxol. *Proc Natl Acad Sci U S A*. 103:10166-73.

Yang, X.J. 2004. Lysine acetylation and the bromodomain: a new partnership for signaling. *Bioessays*. 26:1076-87.

Yang, X.J., and E. Seto. 2007. HATs and HDACs: from structure, function and regulation to novel strategies for therapy and prevention. *Oncogene*. 26:5310-8.

Yang, X.J., and E. Seto. 2008. Lysine acetylation: codified crosstalk with other posttranslational modifications. *Mol Cell*. 31:449-61.

Zhang, D., G.C. Rogers, D.W. Buster, and D.J. Sharp. 2007a. Three microtubule severing enzymes contribute to the "Pacman-flux" machinery that moves chromosomes. *J Cell Biol*. 177:231-42.

Zhang, X., Z. Yuan, Y. Zhang, S. Yong, A. Salas-Burgos, J. Koomen, N. Olashaw, J.T. Parsons, X.J. Yang, S.R. Dent, T.P. Yao, W.S. Lane, and E. Seto. 2007b. HDAC6 modulates cell motility by altering the acetylation level of cortactin. *Mol Cell*. 27:197-213.